Aus der Klinik für Allgemein-, Viszeral- und Transplantationschirurgie,
Klinik (Institut) der Universität München

Vostand Prof. Dr. Jens Werner

Role of Muscarinic Signalling in Pancreatic Cancer

Dissertation
zum Erwerb des Doktorgrades der Medizin
an der Medizinischen Fakultät der
Ludwig-Maximilians-Universität zu München

vorgelegt von
Qian Li

aus
Anshan Liaoning China

Jahr
2022

Mit Genehmigung der Medizinischen Fakultät
der Universität München

Berichterstatter:	Prof. Dr. Jens Werner
Mitberichterstatter:	PD Dr. Georg Beyer
	Prof. Dr. Stefan Böck
Mitbetreuung durch den promovierten Mitarbeiter:	PD Dr. Bernhard W. Renz
Dekan:	Prof. Dr. med. Thomas Gudermann
Tag der mündlichen Prüfung:	30.11.2022

Table of content

Zusammenfassung (Deutsch):

Die Rolle der muskarinischen Acetylcholinrezeptoren in der Tumorigenese wurde bei verschiedenen Krebsarten untersucht. In dieser Studie haben wir die Expression von *CHRM1, CHRM3, CHRM4, CHRM5* und die Expression von CHRM3 und CHRM4 in verschiedenen PDAC-Zelllinien nachgewiesen. Die Rezeptorfunktion wurde anhand des Kalziumflusses und des cAMP-Anstiegs bewertet. Wir konnten nachweisen, dass PDAC-Zellen den funktionellen CHRM3 exprimieren. Die Stimulation von CHRM3 führt zu einem Anstieg des intrazellulären Kalziums in zwei PDAC-Zelllinien mit einem eher epithelialen Phänotyp, wobei DanG-Zellen die empfindlichste Zelllinie in dieser Studie sind. Im Gegensatz dazu führte die CHRM4-Stimulation in unseren Händen nicht zu einem signifikanten Rückgang von cAMP. Darüber hinaus zeigte die CHRM3-Stimulation keine signifikante Auswirkung auf die Viabilität der Zellen. In der DanG-Zelllinie fanden wir jedoch eine eindeutige Untergruppe von Zellen, die CHRM3 exprimierten. Die Zellzyklusanalyse zeigte einen höheren Prozentsatz von CHRM3-positiven Zellen in der Untergruppe der frühen Apoptose (subG1), was die Möglichkeit aufwirft, dass CHRM3 als prognostischer oder Verlaufssparameter in der Behandlung bei PDAC hilfreich sein könnten. Die Analyse der öffentlich zugänglichen ATCC-Datenbank unterstützte diese Hypothese.

Abstract (English):

The role of muscarinic acetylcholine receptors during carcinogenesis has been investigated in different cancer types. In this study, we have shown the expression of *CHRM1, CHRM3, CHRM4, CHRM5*, and the expression of receptor CHRM3 and CHRM4 in different PDAC cell lines. The receptor function was evaluated by calcium flux and cAMP increase. Herein we proved that PDAC cells express functional CHRM3. CHRM3 stimulation can lead to an increase of intracellular calcium in two PDAC cell lines with an epithelial phenotype, DanG cells showed to be the most sensitive cell line in this study. In contrast, CHRM4 stimulation did not induce a significant decrease of cAMP in our hands. Furthermore, CHRM3 stimulation did not reveal a significant effect on cell viability. However, in the DanG cell line, we found a distinct subgroup of cells expressing CHRM3. Cell cycle analysis showed a higher percentage of CHRM3 positive cells in the subG1 early apoptosis subgroup, raising the possibility of CHRM3 being useful as a prognostic or monitoring treatment parameter in PDAC. Analysis of the publicly available ATCC database supported this hypothesis.

List of figures

List of tables

List of abbreviations

WHO	world health organization
HIC	High-Income countries
IHME	Institute for Health Metrics and Evaluation
PDAC	Pancreatic ductal adenocarcinomas
CA 19-9	Carbohydrate antigen 19-9
PNI	Perineural invasion
PanIN	Pancreatic intraepithelial neoplasia
IPMN	Intraductal papillary mucinous neoplasm
ADM	Acinar-to-ductal metaplasia
Shh	Sonic hedgehog
GEMMs	Genetically engineered mouse models
AJCC	American Joint Committee on Cancer
FOLFIRINOX	Fluorouracil, folinic acid, irinotecan, and oxaliplatin
GEM	Gemcitabine
DRG	Dorsal root ganglia
CNS	Central nerve system
DMV	Dorsal motor nucleus of the vagus
NTS	Nucleus tractus solitarius
CHRM1	Cholinergic Receptor Muscarinic 1
CHRM2	Cholinergic Receptor Muscarinic 2
CHRM3	Cholinergic Receptor Muscarinic 3
CHRM4	Cholinergic Receptor Muscarinic 4

CHRM5	Cholinergic Receptor Muscarinic 5
CHRM1	Cholinergic Receptor Muscarinic 1 gene
CHRM2	Cholinergic Receptor Muscarinic 2 gene
CHRM3	Cholinergic Receptor Muscarinic 3 gene
CHRM4	Cholinergic Receptor Muscarinic 4 gene
CHRM5	Cholinergic Receptor Muscarinic 5 gene
G proteins	GTP-binding proteins
cAMP	3'-5'-cyclic adenosine monophosphate
FACS	Fluorescence-activated cell scanning
PCR	Polymerase chain reaction
TCGA	The Cancer Genome Atlas
EFC	Enzyme Fragment Complementation
GPCR	G-protein coupled receptor
RLU	relative luminescence units
EMT	Epithelial to mesenchymal transition
HPAC	human pancreatic cell line
AC	adenylyl cyclase
CHO cells	Chinese Hamster Ovary Cells
ERK	Extracellular-signal-regulated kinase
RAC1	Rac family small GTPase 1
Gq/11	G proteins Gq or G11
PLC	Phospholipase C
PKC	Protein kinase C

1 Introduction

1.1 Pancreatic cancer

1.1.1 Epidemiology

According to the data from the world health organization (WHO), from 2018, pancreatic cancer ranked 15th when calculated the estimated age-standardized incidence rate. High-Income countries (HIC) such as European countries and America tend to have a higher estimated aged-standardized incidence rate of pancreatic cancer (Figure 1). This incidence of pancreatic cancer will keep on rising. In the ranking of the most common cause of cancer-associated deaths, pancreatic cancer will jump to second after lung cancer by the year 2030 in the United States and Germany [1].

Figure 1. The worldwide incidence rate of pancreatic cancer (Data source: GLOBOCAN 2018 Graph production: IARC (http:// gco.jarc.fr/today) World Health Organization)

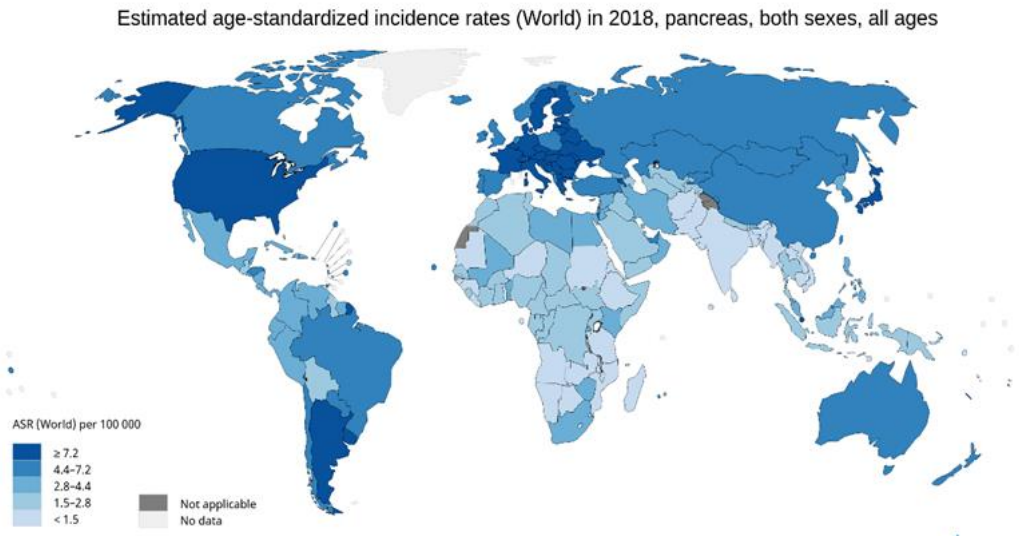

ASR: Age-standardized incidence rates

In terms of morbidity, pancreatic cancer did not show a strong sense of presence. The worldwide new registered case of pancreatic cancer in 2018 was 458,918 which only represents 2.5%

of all cancers [2]. However, pancreatic cancer does bring a big challenge to human society. According to the data from 2017 analyzed by the Institute for Health Metrics and Evaluation (IHME), around 0.01% of the population in Germany lives with pancreatic cancer, it is on rank 18 among all different cancer types, but when focusing on disease burden rates it comes to the top 4 (Figure 2. A, B). This difference reminds people how terrifying this disease could be.

Figure 2. The overview of cancer in Germany.

A,

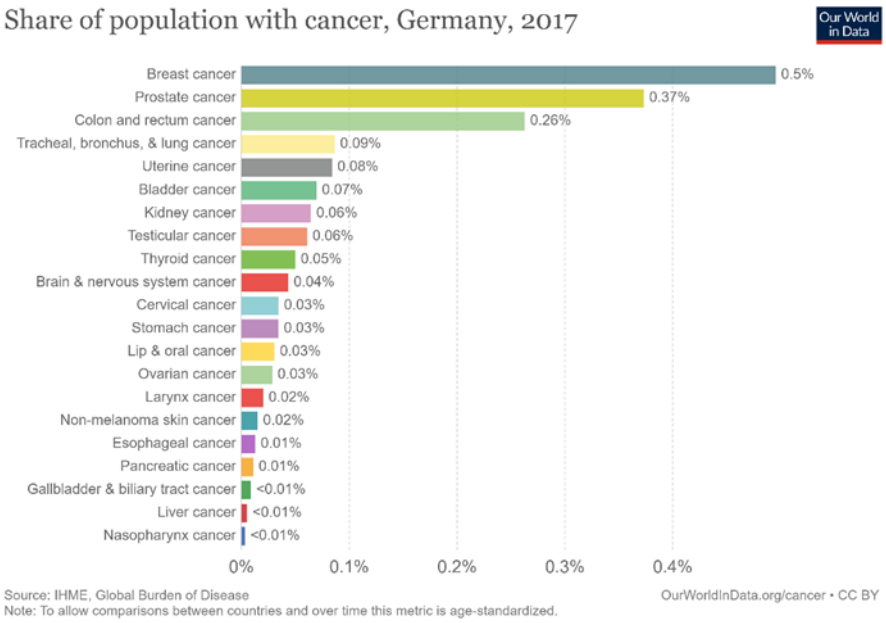

B,

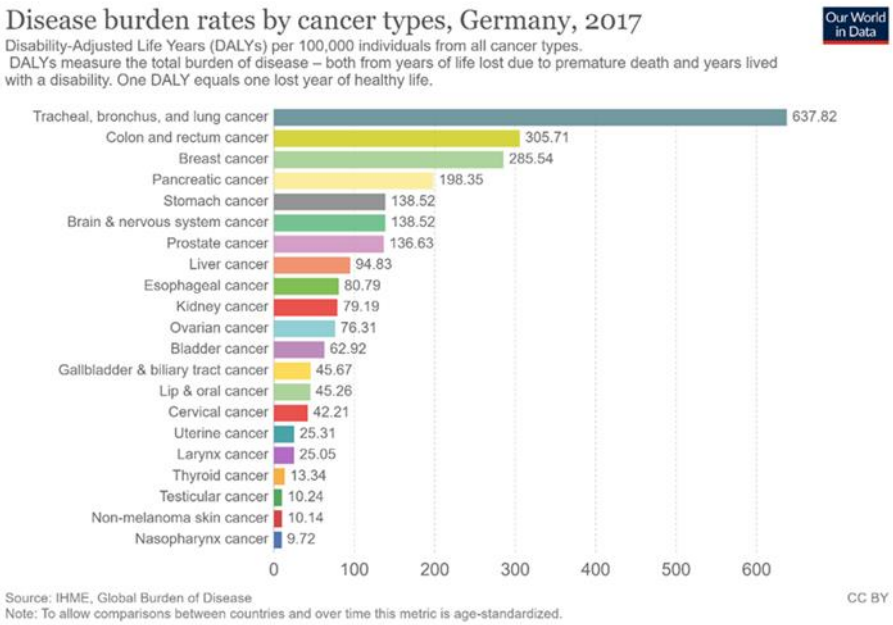

1.1.2 Diagnostics of pancreatic ductal adenocarcinomas (PDAC)

Pancreatic cancer comprises all neoplasms that arise from the pancreas. These pancreatic neoplasms have a broad spectrum and are classified by histological differentiation and biological behavior. Pancreatic ductal adenocarcinomas (PDAC) which arise from the exocrine glands and ductular cells of the pancreas are accountable for 85% of all pancreatic neoplasms.

The early symptoms of PDAC are insidious. Some non-specific symptoms like anorexia, early satiety, or asthenia are often missed, abdominal pain is also missing. As the disease progresses, patients may suffer digestive insufficiency, weight loss, or paraneoplastic thromboembolic events. New-onset diabetes or malnutrition is also common when there is cancer-associated pancreatic insufficiency. When there is a suspected PDAC case, a pancreatic protocol computer tomography (CT-scan) and the Carbohydrate antigen 19-9 (CA 19-9) level are early clinical diagnostic tools. When the tumor is located in the pancreatic head, the appearance of jaundice can be an early clinical sign due to compression of the intrapancreatic bile duct.

Neuropathy is a hallmark feature in PDAC. The incidence of Perineural invasion (PNI) is as high as 80%-100% and therefore higher than in most solid tumors. Due to this fact, the typical pain during PDAC progress is neuropathic. It is commonly described as severe abdominal pain radiating toward the back. Different from somatic pain and visceral pain, neuropathic pain is caused by the perineural invasion of retro-pancreatic nerves. The pathophysiology for this neuropathic pain might be the cancer cell invasion associated nerve damage which leads to growth stimulation of sensory fibers. During this nerve repair process, an increase in neuroplasticity and neuropathic pain immerges [3,4]. The severity of neural invasion is also associated with a worse prognosis [5].

1.1.3 The origin of PDAC

Like other cancers, PDAC also arises from precursor lesions, including pancreatic intraepithelial neoplasia (PanIN) and intraductal papillary mucinous neoplasm (IPMN).

Pancreatic intraepithelial neoplasia (PanIN) is believed to be the precursor lesions for the vast majority of PDACs [6]. The transform from PanIN to invasive PDAC can be divided into 3 different stages from lower to a higher grade, which are PanIN-1, PanIN-2, and PanIN-3. According to research, in the healthy pancreas, there is no PanIN-3, but in the case of chronic pancreatitis, 4% of all cases have PanIN-3. The morbidity further increases in pancreatic cancer patients, 40% of these patients harbored a PanIN-3 lesion [7]. Morphologically, the PanIN lesions show cytologic and architectural atypia, and the degree of dysplasia is gradually enhanced from PanIN-1 to PancIN-3. The PanIN-1 lesions have two types: flat (PanIN-1A) and papillary (PanIN-1B). The size of PanIN-1 is small (<0.5 cm in diameter), under the microscope, they present as flat or papillary noninvasively epithelial neoplasms with ductular phenotype. PanIN-2 lesions have a more complex architecture, cell nuclear began to lose the polarity, combine with the emerge of other nuclear changes like crowing, pleomorphism, hyperchromasia, and pseudosrtratification [8]. PanIN-3 lesions have more advanced dysplasia, a typical structure of the gland becomes rare, and cribriform structures forms. The cells show higher invasiveness ability behaver as breakthrough the basal layer and growing into the lumen of the duct. Cytologically, during PanIN-3, there are more obvious morphological changes in the nucleus. Widely emerge cells whose nucleus are enlarged, pleomorphic, and poorly oriented, a more prominent of mitotic figures or even abnormal mitosis in nucleoli [8].

The origin of PDAC is quite controversial. There are three major epithelial cell types in the pancreas, which are acinar, duct and islet cells. According to the existing research, the acinar and duct cells both have the potential to form pancreatic ductal adenocarcinoma. The acinar cell is a kind of terminally differentiated cell which synthesizes, stores and secretes pancreatic digestive enzymes. These cells are normally postmitotic and mitotically quiescent. However, when there is a chronic injury accompanied by inflammation that happens to pancreatic tissue, the acinar cells undergo a metaplastic process that can reverse the postmitotic and differentiated cell fate, the cell shape change into duct-like structures, this process is called acinar-to-ductal metaplasia (ADM). ADM is a common and reversible pathological process during pancreatitis. This has already been shown in both mouse and human tissue [9,10]. However, the transition from ADM to PDAC in humans is still under investigation. Studies in mouse acinar cells and transgenic mouse

models show that ADM becomes irreversible after cells having acquired an oncogenic *Kras* mutation. On the other hand is a *Kras* mutation in mice not sufficient to develop full blown cancer, without further events as inflammation or acquisition of additional gene mutations ("2nd hit") [11–13]. By now, only under such conditions, the ADM cells show the ability to give rise to PanIN [14].

Pancreatic duct cells are epithelial cells from branched tubes that deliver pancreatic acinar cells produced enzymes into the duodenum. These cells can also be transformed and therefore progenitors of Intraductal Papillary Mucinous Neoplasms (IPMN). The IPMN is characterized by ductal dilation with intraductal papillary proliferation and thick mucus secretion. There are four types of IPMN, which are gastric type, intestinal type, pancreaticobiliary type, and oncocytic type [15]. Most IPMN derived PDAC are developed from the intestinal type instead of the gastric type, while the other two types are usually malignant lesions [16].

A study using genetically engineered mouse models (GEMMs) shows, that acinar cells were much more susceptible to transformation than ductal cells [16]. This study led to the conclusion that the pancreas acinar cells are more likely the cell type of origin for pancreatic cancer in mice. However, the situation in human PDAC is less clear.

Figure 3. The process of PDAC oncogenesis (Adapted from Ref. [17]).

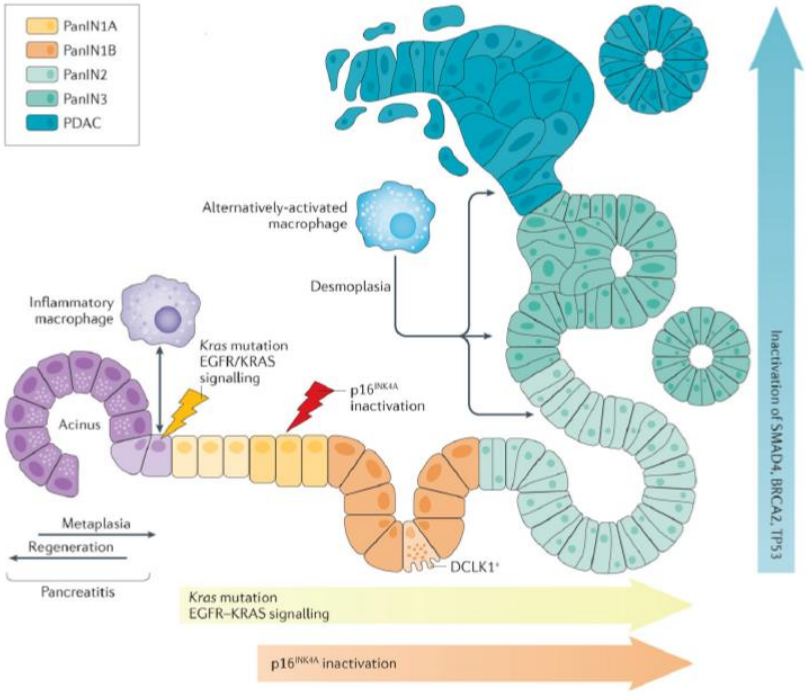

1.1.4 Treatment for PDAC

A multidisciplinary approach is recommended for PDAC treatment. The strategy may combine surgery, chemotherapy, and chemoradiotherapy. Also, supportive care is necessary for the patients who are suffering from challenges of physical, practical, and emotional conditions.

For PDAC, surgical treatment is still the only potentially curative option. A careful evaluation and pretherapeutic staging have to be carried out for the selection of suitable surgical candidates. The surgical options for PDAC normally include partial pancreatoduodenectomy (Whipple procedure), distal pancreatectomy, and in selected cases a total pancreatectomy. A partial pancreatoduodenectomy is recommended when the tumor is located in the head of the pancreas. During the operation, the head of the pancreas, the duodenum, the gallbladder, and the bile duct will be resected. A distal pancreatectomy is recommended for patients with adenocarcinoma in the body or tail of the pancreas. The surgical resection part involves the body and tail of the pancreas [18].

During operation, harvesting of at least 15 lymph nodes is recommended [19]. The margin of the posterior pancreatic surface, superior mesenteric vein, and medial margin are examined and reported according to the standardized pathological protocol from American Joint Committee on Cancer (AJCC). The definition of tumor clearance is the precise distance between the tumor cells and the margin [20]. The microscopically negative margins (R0) are defined as the margin of the removed tumor and the healthy tissue larger than 1mm. If R0 cannot be achieved, it should be distinguished between a tumor-free margin less than1 mm (R1(<1 mm)) and tumor cells detect on the margin (R1 (direct)). A tumor cell positive margin indicates a worse prognosis [21].

Adjuvant chemotherapy for physically fit patients consists of FOLFIRINOX (Fluorouracil, Folinic acid, Irinotecan, and Oxaliplatin) or Nab-paclitaxel and Gemcitabine (GEM). For patients older than 75, single-drug therapy of GEM is recommended. Chemotherapy can only provide a dramatically improved outcome for those patients with resectable disease, once the tumor is spread the benefit becomes limited [22].

1.2 The involvement of the nerve system in PDAC

1.2.1 The pancreatic innervation

The pancreas is innervated by nerve fibers originating from the ventral plexus. There are three qualities of never fibers present in the pancreas, sensory, sympathetic, and parasympathetic.

The spinal and vagal pathways are the main route for the transmission of the pancreas sensory information. The T6-L2 dorsal root ganglia (DRG) contain the cell body of the spinal afferent pancreatic neurons, the axons traverse through the splanchnic nerve and celiac plexus, then enter the pancreas. These sensory nerve fibers transmit the mechanoreceptive and nociceptive information to the central nerve system (CNS) through the preganglionic sympathetic neurons [23,24].

The sympathetic preganglionic neurons are located in different segments of the spinal cord, from the lower thoracic segments T5 to the upper lumbar segment T9. The sympathetic axons that leave the spinal cord are then divided into two branches, one supplies the paravertebral ganglia of the sympathetic chain while the other supplies the celiac and mesenteric ganglia. The postsynaptic catecholaminergic neurons of these ganglia innervate islet, blood vessels, intrapancreatic ganglia, and to a lesser extent the exocrine unit of the pancreas [25].

The parasympathetic nervous system of the pancreas is better studied, it is now clarified that the effect of this nervous system is mainly focused on the regulation of the exocrine function. The preganglionic parasympathetic neurons arise from the dorsal motor nucleus of the vagus (DMV) which receives signals from the adjacent nucleus tractus solitarius (NTS) and the area of postrema and hypothalamic, also the higher-order neurons like the prefrontal, piriform and gustatory cortices. This wide connection in the CNS supports the existence of the cephalic phase of exocrine secretion [26]. The parasympathetic nerves combine with a part of sensory nerves, before entering into the pancreas. In the pancreas, parasympathetic nerves also show a wider distribution than sympathetic and sensory nerves. The parasympathetic innervation has a higher density in the head and neck of the pancreas, but also has a wide distribution in the rest of the

pancreas. Due to the sensory nerve fibers component, the vagus nerve can influence the pancreatic endocrine secretion. However, the more crucial role of the vagus nerve is the regulation of pancreatic exocrine secretion[27].

Figure 4. The Neuroanatomy of the pancreas (Netter's Neuroscience Flash Cards).

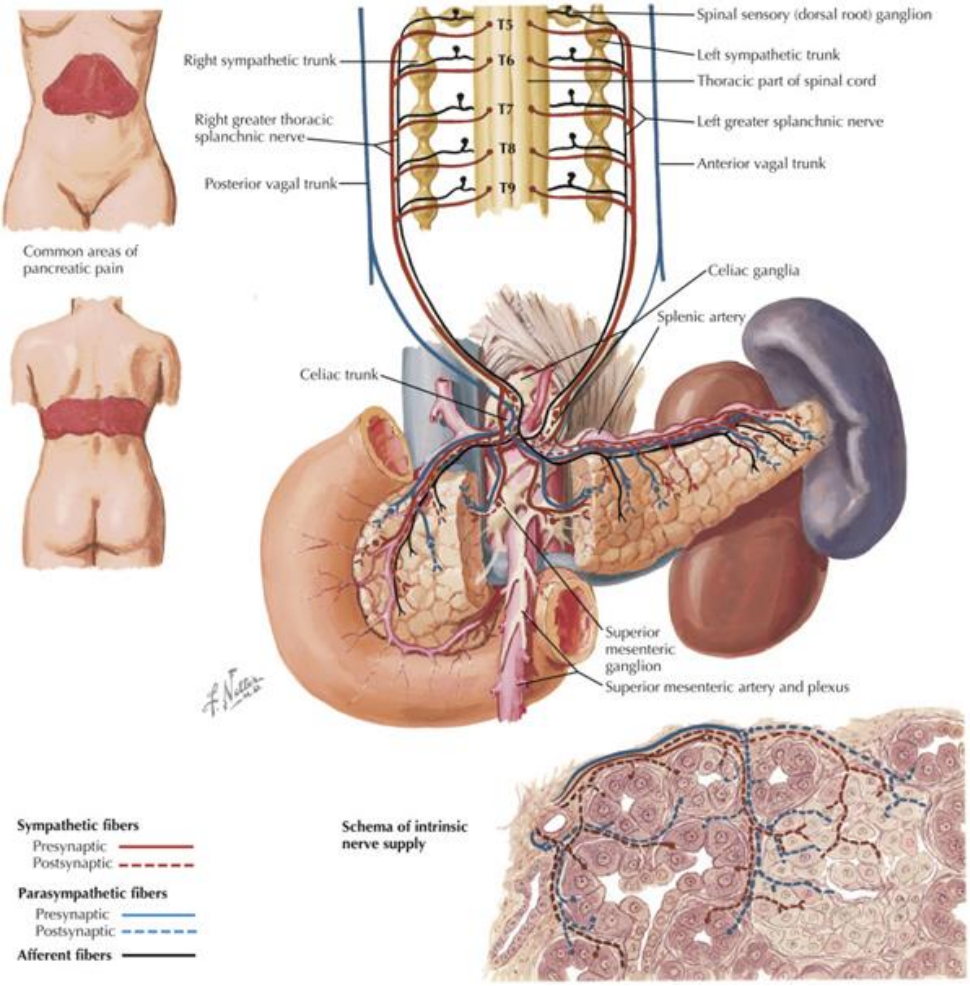

1.2.2 Neuropathy in PDAC

During PDAC progression, cancer-associated neuropathy is very common phenomenon, histologically manifested as perineural invasion. The pancreatic cancer cells invade the perineurium

of the neuronal sheath, enter into the endoneurium spaces. Those involved pancreatic nerve fibers undergo neural remodeling processes. Intriguingly, in PDAC neural density and size are significantly increased. These changes are described as neural hypertrophy [28].

There is a positive correlation between the severity of perineural invasion and patient survival. For patients who have survived longer than 3 years after surgical resection, the extrapancreatic nerve invasion was all negative at the time of surgery [29]. Not only in pancreatic adenocarcinoma but other gastrointestinal tumors, neural invasion indicates aggressive tumor behavior and is involved in tumorigenesis and progress (Table 1).

Table 1. The incidence of PNI in different digestive system tumors

Cancer type	Percentage of PNI patients (%)	Effect on survival	Refs.
Pancreatic ductal adenocarcinoma	70-100	Shorten the OS	[30–32]
Gastric carcinoma	60	Shorten the OS	[33]
Colorectal cancer	33	• Shorten the Five-year OS; • Decrease the five-year disease-free survival	[34]

1.2.3 The cholinergic nerve system in pancreatic cancer progression

As mentioned above, the pancreas is innervated by nerves with qualities. The density and distribution of sympathetic, sensory, and parasympathetic nerve fibers have significant tissue variance, even in different parts of the same organ. Along these lines, studies in different cancers entities have been carried out and provide a further understanding of neural regulation in cancer (Table 2).

Table 2. Effect of different peripheral nervous systems in different digestive system tumors.

Cancer type	Protumorigenic nerve system	Antitumorigenic Nerve system	Refs.
Pancreatic cancer	• General innervation • Sympathetic Sensory	Parasympathetic	[35–39]
Gastric cancer	Parasympathetic	Sympathetic	[33,40]
Colon cancer	General innervation	Parasympathetic	[41–43]

In pancreatic cancer, previous studies have shown a cancer-promoting effect of sensory nerves and sympathetic nerves. This effect is mainly attributed to Substance P signaling and adrenergic signaling [35,37]. Recently it was shown that cholinergic signaling can inhibit pancreatic tumor progression [36]. According to the data, this effect is mediated by the muscarinic receptor M1 (CHRM1) on pancreatic cancer cells, which is in contrast to the results of previous denervation experiments in prostate and gastric cancer [33,44]. The vagus nerve is composed of 80% sensory nerve fibers and 20% parasympathetic nerve fibers. Although the cancer-promoting effect of sensory nerves on pancreatic cancer has already been reported, the overall effect of parasympathetic nerve fibers seems to be tumor-suppressive [37]. This stresses the complexity of a tumor-neuronal cross-talking.

Acetylcholine is the main neurotransmitter of the parasympathetic nervous system and signals through nicotinic and muscarinic receptors. For nicotinic receptors, a PDAC promoting effect has been already shown [38]. The tumor-suppressive effect of muscarinic receptors mentioned above, shows that the receptor subtype is important. Furthermore, other types of cells in the tumor microenvironment also express muscarinic and nicotinic receptors. Therefore, an indirect effect on tumor regulation is also possible.

There are five subtypes of the muscarinic receptor, named cholinergic receptor muscarinic 1to 5 (CHRM1-5). All these muscarinic receptors are GTP-binding proteins (G proteins) coupled receptors. CHRM1, CHRM3, and CHRM5 belong to the Gq/11 family, receptor activation led to the activation of phospholipase C and the increase of cytosolic Ca^{2+}. CHRM2 and CHRM4 belong

to the Gi/o family, causing the inhibition of adenylyl cyclase, leading to a decrease of intracellular adenosine 3′,5′-cyclic monophosphate (cAMP) concentrations (Figure 5) [45].

Figure 5. The activation mechanism of the Muscarinic receptor

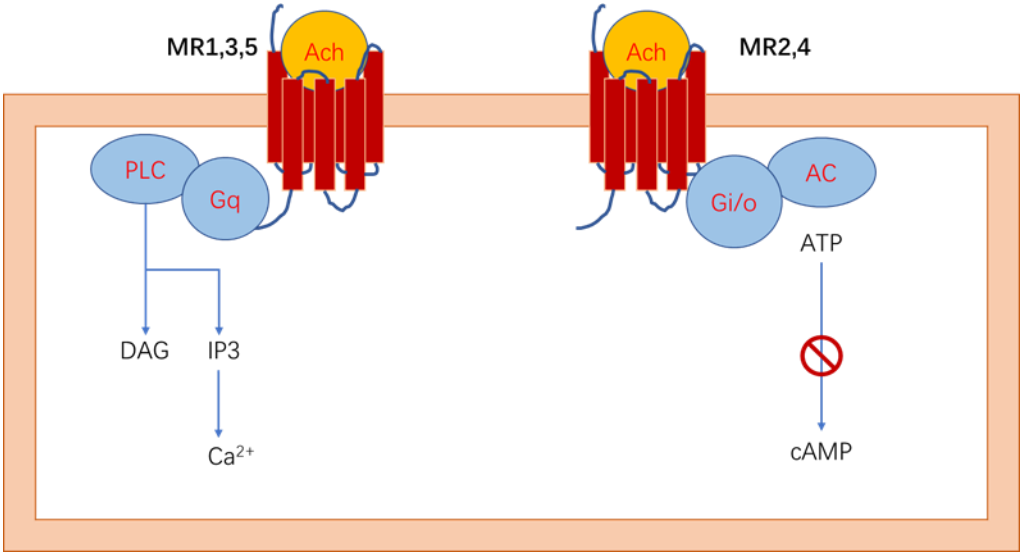

Different kinds of cancer cells can express functional muscarinic receptors, and these receptors can have influences on tumor progression (Table 3). As expected, these studies show that the effect of muscarinic receptor activation depends on the cellular phenotype and receptor subtypes. For instance, activation of the CHRM3 receptor can induce proliferation in prostate carcinoma cells but can inhibit DNA synthesis in small cell lung carcinoma [46,47]. Although CHRM1 has already been proven inducing a cancer inhibitory effect, there are also data reporting that pancreatic tumors are significantly promoted after an *in vivo* muscarinic receptor agonist treatment [36]. The specific subtype of the muscarinic receptor involved was not investigated [48].

Table 3. The studies of Muscarinic receptor effect in different cancers.

	Tumor type	Muscarinic Receptor involved	Biological influence	Refs.
Enhancement effect on tumor	Melanoma	CHRM3, CHRM5	Enhance cell migration	[49]
	Colon cancer	CHRM3	Enhance proliferation	[50]
	Small cell lung carcinoma (SCLC)	CHRM3	Enhance proliferation	[51]
	Prostate cancer	CHRM1	Enhance migration and invasion	[46]
		CHRM3	Enhance proliferation	[46]
	Breast cancer	CHRM2, CHRM3	Enhance proliferation	[52,53]
	Mammary Adenocarcinoma	CHRM3	• Enhance proliferation • Angiogenesis	[54]
	Astrocytoma	CHRM3	Enhance proliferation	[55]
	Oral cancer	CHRM4	Enhance cell migration	[56]
Inhibition effect on tumor	Glioblastoma	CHRM2	Inhibited cell proliferation	[57]
	Pancreatic cancer	CHRM1	Inhibited cell proliferation	[36]
	Neuroblastoma	CHRM1	Inhibited cell proliferation	[58]
	Astrocytoma	CHRM3	Inhibited cell migration	[55,59]

The nerve network may influence the tumor microenvironment. The effect might be direct or indirect. When there is a direct effect, the muscarinic receptor may work as one of the first line signals between neurons and cancer cells. Knowing the distribution of different subtypes of muscarinic receptors on PDAC cells, and the biological behavior between different receptor expressing cell populations, may give us a better understanding of the role of the muscarinic receptor during PDAC progress.

1.3 Aim

As there is a lack of understanding regarding the different muscarinic receptors in PDAC, this study aimed to investigate expression levels and biological relevance of muscarinic receptor subtypes in different human pancreatic ductal adenocarcinoma cell lines and pancreatic cancer tissue. Furthermore, the expression levels will be correlated with PDAC patients' survival.

2 Material and Methods

2.1 Materials

2.1.1 Consumables

Consumables	Source
6-well plate	Nunclon™ delta surface
12-well plate	Nunclon™ delta surface
24-well plate	Nunclon™ delta surface
96-well plate	Sarstedt
5 mL Pipette	Costar
10 mL Pipette	Costar
25 ml Pipette	Costar
1.5ml tip	Eppendorf
2.0ml tip	Eppendorf
15ml tube	TPP
50ml tube	Falcon
Blot paper	Bio-Rad
Cell culture flask T25	Nunclon™ delta surface
Cell culture flask T75	Nunclon™ delta surface
Cell culture flask T125	Nunclon™ delta surface
Cell scraper	TPP
FACS tube	Falcon
Filters 0.25ul	Sartorius stedim
Filters 0.45ul	Sartorius stedim
QIAshredder spin column	Qiagen
Glass coverslips	Menzel Gläser

Glass slides	Marienfeld
PVDF transfer membrane	Thermo
96-Well White, Clear Flat-Bottom, TC-Treated, Sterile Plates with Lid	DiscoverX
Sterile needle	BD Microlance ™

2.1.2 Chemicals

Chemicals	**Source**	**Identifier**
β-Mercaptoethanol	Sigma	M6250
Agarose	Peqlab	35-1020
Ammonium persulfate (APS)	Serva	13376.01
BSA	Biomol	01400.100
Crystal violet	Sigma	C0775
6x DNA Sample Loading Buffer	Thermo	R0611
DMSO	Sigma	D2650
1 Kb Plus DNA Ladder	Invitrogen	10787-018
ECL™ Western Blotting Detection System	Amersham Biosciences	RPN2209
70% ethanol	Pharmacy	T868.1
FBS	Sigma	F7524
SYBR Safe DNA Gel Stain	Invitrogen	S33102
Precision Plus Protein™ Dual Color Standards	BIO-RAD	#161-0394

Isopropanol	Roth	UN1219
Loading buffer 4x	Bio-Rad	161-0747
Methanol	Merck	1.06009.1000
Milk powder	Roth	T145.2
PBS	PAN-Biotech	P04-36500
IC Fixation buffer	eBiosciences	00-8222-49
Penicillin-Streptomycin	Lonza	DE17-602E
Permeabilization Buffer 10x	eBiosciences	00-8333-56
Phosphatase inhibitor cocktail	Roche	04906837001
Protein standards	Bio-Rad	161-0374
Protease inhibitor cocktail	Roche	05892791001
RNase-free water	Qiagen	129112
RPMI 1640 Medium	Gibco™	21875-034
RIPA lysis buffer 10x	Millipore	20-188
SDS	Carl Roth	2326.2
SYBR safe DNA gel stain	Invitrogen	S33102
TAE buffer 50x	SERVA	42549.01
TEMED	Bio-Rad	161-0800
Tris Base	Bio-Rad	161-0716
Triton-X-100	Sigma	T8787
Trypan blue	Sigma	T8154
Trypsin/EDTA	Lonza	BE17-161E
Tween 20	Sigma	P1379
Magnesium sulfate-Heptahydrate	Merck	10034-99-8
Calciumchlorid-Dihydrate	Merck	10035-04-8
Pluronic F-127 20% solution in DMSO	Invitrogen	P3000MP

Versene	Gibco™	15040066

2.1.3 Antibodies

Antibodies	Source	Identifier
Rabbit anti-M4 Muscarinic Receptor Antibody	Alomone Labs	AMR-004
GAPDH(D16H11) XP Rabbit mAb	Cell Signaling	#5174
Anti-rabbit IgG, HRR-linked Antibody	Cell Signaling	#7074
Muscarinic Acetylcholine Receptor M3 antibody	Novus Biologicals	NBP2-19444
Rabbit IgG Isotype Control	Novus Biologicals	AB-105-C
Rabbit IgG APC-conjugated Antibody	Novus Biologicals	F0111

2.1.4 Agonist and Antagonist

Product	Source	Identifier
Carbachol	Sigma-Aldrich	Y0000113
Darifenacin hydrobromide	Sigma-Aldrich	SML1102
Forskolin	DiscoverX	92-0005
Ionomycin calcium salt	Sigma-Aldrich	I0634
Isoprenaline hydrochloride	Sigma-Aldrich	I0599990

2.1.5 Commercial Assays

Product	Source	Identifier
Pierce™ BCA Protein Assay Kit	Thermos fisher	#23225
Human brain tissue-derived BioBank cDNA	Primer Design	cDNA-hu-ti C0166
Clarity Max™ Western ECL Substrate	BIO-RAD	#1705062
RNeasy Mini Kit	Qiagen	74106
QuantiTect Reverse Transcription Kit	Qiagen	205311
QuantiFast SYBR Green PCR Kit	Qiagen	204056
HitHunter® cAMP Assay for Small Molecules	DiscoverX	90-0075SM2
BD Pharmingen™ BrdU Flow Kits	BD	559619
Indo-1, AM, cell permeant - Special Packaging	Invitrogen	I1223
EZ4U kit	Biomedica	BI-5000

2.1.6 Primers

Primers	Source	Identifier
CHRM1	Qiagen	QT00215404
CHRM2	Qiagen	QT00092134
CHRM3	Qiagen	QT00200354
CHRM4	Qiagen	QT00214963
CHRM5	Qiagen	QT00206346

β-actin	Qiagen	QT00095431

2.1.7 Apparatus

Apparatus	**Company**
Autoclave	Unisteri
AxioCam MRC5	ZEISS
Centrifuge	Hettich
Cool Centrifuge	Eppendorf
Microcentrifuge	Labtech
CO_2 Incubator	Binder
DNA workstation	Uni Equip
Drying cabinet	Heraeus
Electronic pH meter	Knick
FACS Fortessa	BD Biosciences
4°C Fridge	Siemens
- 20°C Fridge	Siemens
-80°C Fridge	Siemens
Thermomixer	eppendorf
Ice machine	KBS
Liquid Nitrogen tank	MVE
Lamina flow	Heraeus flow laboratories
Microscope	Olympus
Microwave Oven	Siemens
Micro weigh	Chiyo
Nanodrop 2000	Peqlab
Step one PCR system	Applied Biosystems
Pipette controller	Eppendorf

Microplate reader	VERSA max
Microplate reader	FilterMax F3
Power Supply Power Pac 300	BIO-RAD
Power supply	Novax PowerEase 500
Shaker	Edmund Bühler
Mini-trans blot electrophoretic transfer cell	BIO-RAD
5331 Master Cycler Gradient Thermocycler	Eppendorf
Thermomixer comfort	Eppendorf
X cell II TM Blot module	Invitrogen
Vortex	Janke Kunkel
Water bath	Memmert
UV illuminator	Labor Technik
Hypercassette	Amersham Biosciences
ChemiDoc MP Imaging System	BIO-RAD

2.1.8 Solutions

- Indo-1 store solution (2mg/ml): 50µg indo-1 + 25 µL Pluronic F-127 20% solution in DMSO
- Cell loading media for Indo-1 assay (1mM Mg^{2+},1mM Ca^{2+},0.5%BSA): 250ml DPBS+ 0.067g $MgSO_4.7H_2O$+0.039g $CaCl_2.2H_2O$+1.28g BSA
- FACS buffer: 1L 1x DPBS + 2ml Natriumacid+ 5g BSA
- 1 M TRIS (for stacking gel): 12,1 g TRIS + 100 ml with VE-H2O, adjust the pH to 6,8 (use

HCl)

- 1,5 M TRIS (for separating gel): 18,21 g TRIS + 100 ml with VE-H2O, adjust the pH to 6,8 adjust the pH to 8,5 (use HCl)
- 10x electrophoresis buffer: 30 g TRIS Base +144 g Glycin +10 g SDS +1 L VE-H2O. For following dilution 1x 100 ml buffer + 900 ml VE-H2O
- 10x Blotbuffer: 15 g Glycin +144 g TRIS +1 L VE-H2O. For following dilution 1x 100 ml Puffer + 100 ml Methanol + 800 ml VE-H2O
- 10x TBS: 24 g TRIS Base +80 g NaCl +1 L VE-H2O
- 1x TBS-T: 100 ml 10x TBS + 900 ml VE-H2O + 1 ml Tween (pH 7,6)
- Blocking buffer (5% milk): 0,5 g dried milk + 10 ml TBS-T
- 5% BSA for dilution of antibodies: biotin-free BSA 0,5 g +10 ml TBS-T
- Western blot Separating gel: H_2O 4,3ml + 1,5M TRIS (pH 8,5) 2,5ml+ Polyacrylamide 3ml + 10% SDS 100µl + 10% APS 100µl+ TEMED 5µl
- Western blot Stacking gel: H_2O 2,3ml + 1M TRIS (pH 6,8) + 380µl Polyacrylamide 380µl + 10% SDS 30µl + 10% APS 30µl+ TEMED 5µl

2.1.9 Software

- GraphPad Prism (ver 5.0, GraphPad Software Inc, La Jolla, CA, USA).
- SoftMax® Pro Microplate Data Acquisition and Analysis Software (Version 6.5.1).
- BD FACSDiva™ Software v8.0
- ImageJ (FIJI)

2.2 Method

2.2.1 Cell culture conditions and routine cell culture

Pancreatic cancer cell lines (BxPc3, DanG, Panc1) were cultured with RPMI1640 medium supplemented with 10% FBS (Fetal Bovine Serum) and 1% P/S (Penicillin/Streptomycin). Culture Condition was 95% air atmosphere, 5% carbon dioxide (CO2), 37°C. The sub-cultivation ratio was 1:4 with 2 times subculture per week. Before subculturing the cell has around 80% confluence, aspirated all the medium, washed with Dulbecco's PBS 1 time then added Trypsin-EDTA and gently rocked to ensure complete coverage over the cells. Incubated for 5 minutes at 37°C, after ensuring the majority of cells were detached, add an equal volume of the complete medium into the flask to neutralize the trypsin-EDTA, pipette to ensure cells were dissociated from each other. Transferred the cell suspension to a 50mL centrifuge tube, centrifuged at 500 g x for 5 minutes. Resuspend the cell pellet in the pre-warmed fresh complete medium then seed in the new Flask at an appropriate cell density. Renew the culture media every 2 days. The volume of Trypsin-EDTA and culture medium was summarized and shown in Table 4.

Table 4. Volumes of Dulbecco's PBS, Trypsin-EDTA, and Medium used in cell passage.

Culture Wares	Trypsin-EDTA	Dulbecco's PBS	Medium
6- well plate	0.5 mL / well	0.5mL	3.0 mL / well
T-25 flask	1.0 mL / flask	1mL	5.0 mL / flask
T-75 flask	3.0 mL / flask	5mL	10.0 mL / flask
T-175 flask	5.0 mL / flask	10mL	20.0 mL / flask

2.2.2 mRNA isolation and concentration measurement

$0.5x10^6$ cells were seeded and cultured in 6 wells plate for 48 hours, total mRNA was isolated from the cell pellet using the RNeasy Mini Kit (Qiagen). Harvested $1x10^6$ cells and then centrifuged for 5 minutes at 300 x g in a centrifuge tube, removed all supernatant by aspiration. loosen the cell pellet thoroughly by flicking the tube, adding 350 µL Buffer RLT, and mixing by vortexing. To

homogenize the lysate, piped the lysate directly into a QIAshredder spin column placed in a 2ml collection tube, and centrifuged for 2 minutes at full speed. Added 350 µL of 70% ethanol to the homogenized lysate, and mixed well by pipetting. Transferred 700 µl of the sample to a RNeasy spin column placed in a 2ml collection tube, closed the lid gently and centrifuged for 15 seconds at 8000 x g, discard the flow-through. Added 700 µl Buffer RW1 to the RNeasy spin column, centrifuged for 15 seconds at 8000 x g to wash the spin column membrane. Added 500 µl Buffer RPE to the RNeasy spin column and centrifuged for 15 seconds at 8000xg to wash. Added 500 µl Buffer RPE to the RNeasy spin column, then gave a 2 minutes long centrifugation at 8000xg to ensure that no ethanol is carried over during RNA elution. Placed the RNeasy spin column in a new 1.5 ml collection tube, added 30 µl RNase-free water directly to the spin column membrane, centrifuged for 1 minute at 8000 x g to elute the RNA. The mRNA concentration was measured by Nanodrop 2000 (Peqlab). mRNA samples were stored in a -80°C fridge for longer storage.

2.2.3 Reverse Transcription

The mRNA sample was reverse-transcripted using QuantiTect Reverse Transcription Kit (Qiagen) according to the manufacturer's protocol. The genomic DNA elimination reaction was performed before the reverse transcription, the reaction components were shown in Table 5, incubated the reaction components mix for 2 minutes at 42°C to eliminate the genomic DNA.

Table 5. Genomic DNA elimination reaction components

Component	**Volume/reaction**	**Final concentration**
gDNA Wipeout Buffer, 7x	2 µl	1x
Template RNA	The volume of 1 µg mRNA *	
RNase-free water	14 µl – the volume of template RNA	
Total volume	**14 µl**	

* Volume is depending on the concentration of the Template RNA.

The reverse-transcription master mix was performed on ice according to Table 6, The master mix was incubated for 15 minutes at 42°C to generate the reaction, then further incubated for 3 minutes at 95°C to deactivate the Quantiscript reverse transcriptase.

Table 6. Reverse-transcription reaction components

Component	Volume/reaction	Final concentration
Reverse-transcription master mix		
Quantiscript Reverse Transcriptase	1 µl	
Quantiscript RT Buffer, 5x	4 µl	1x
RT Primer Mix	1 µl	
Template RNA		
Entire genomic DNA elimination reaction	14 µl (1 µg)	
Total volume	**20 µl**	

All the incubation steps for the Genomic DNA elimination reaction and Reverse-transcription reaction were performed using the PCR cycler (Eppendorf).

2.2.4 Quantitative real-time polymerase chain reaction (qPCR)

cDNA obtained from mRNA reverse transcription was used in the qPCR added with the primer of *CHRM1, CHRM2, CHRM3, CHRM4, CHRM5,* and *β-actin* from QuantiTect® Primer Assay (Qiagen). The positive control sample was the cDNA sample from human brain tissue which is a commercial BioBank cDNA kit (Primer Design), the Quantitative real-time PCR was performed with QuantiFast SYBR Green PCR Kit (Qiagen) using Step one PCR system (Applied Biosystems) and PCR System Software (StepOne™ software). The reaction setup shows in Table 7. All the qPCR reactions were done in triplicate and the protocol used was: hot start for 10 minutes at 95°C, followed by 45 cycles of 15 seconds at 95°C, annealing for the 30 seconds at 55°C and

extension for 30 seconds at 72°C. Data were normalized with housekeeping gene *β-actin*, ΔΔCt method was used to calculate the fold changes in the gene expression, as compared to the control group.

Table 7. Reaction setup for qPCR

	Volume/reaction	
Component	**96-well block**	**Final concentration**
2x QuantiFast SYBR Green PCR Master Mix	12.5 µl	1x
10x QuantiTect Primer Assay	2.5 µl	1x
Template cDNA	1 µl	100ng/reaction
RNase-free water	9µl	
Total volume	**25 µl**	

2.2.5 DNA electrophoresis

Prepare 1.5 % agarose gel with 1.5 g agarose (Peqlab) and 100mL 1xTAE buffer (SERVA), Melt the agarose mixture solution by heating in a microwave until the agarose has completely dissolved. Before the gel is poured, added 20 µl of SYBR Safe DNA Gel Stain (Thermo Fisher Scientific) for nucleic acid staining, mixed well by panning. Pour the gel into the gel carrier and allow the gel to harden with the length and width of 131mm x 60mm respectively, each sample well was 5 mm. During electrophoresis, prepare each sample by mixing 25µl qPCR product with 5µl 6X DNA Sample Loading Buffer (Thermo), prepare1 Kb Plus DNA Ladder (Invitrogen) with 6.5 µl molecular biology H_2O mixed with 1.5 µl 6x Loading buffer and 1 µl DNA ladder. Pour 1xTAE buffer into the chamber and load the gel with the prepared samples. For each sample and the DNA ladder, apply 10 µl to the agarose gel. The DNA electrophoresis program was 60 minutes, 100V, 200mA, 50W, power supply by Power ease500 Thermo Fisher Scientific.

2.2.6 Protein isolation

Scraping the cells from a 6-well plate, the cell lysates were obtained using 1x RIPA lysis Buffer (Millipore) containing a cocktail of protease and phosphatase inhibitors (Roche). Cell lysates were incubated on ice for 10 minutes then collected with a 1.5mL tube, centrifuged for 15 minutes at 14,000 x g at 4°C, the supernatant was collected in a new tube. Protein samples were stored in a -20C° fridge for longer storage.

2.2.7 Protein concentration measurement (BCA Protein Assay)

Protein concentration was determined using the Pierce™ BCA Protein Assay Kit (Thermos Fisher). Setting up a group of controlled samples with a working range from 25 to 2,000µg/mL by diluting the contents of one Albumin Standard (BSA) ampule into several clean vials, to create a standard curve. Prepared the BCA working reagent by mixing 50 parts of BCA Reagent A with 1 part of BCA Reagent B. Pipetted 25µL of each controlled sample or 1:5 diluted unknown sample replicate into a 96-well microplate. Added 200µL of BCA working reagent to each well and mixed plate thoroughly on a plate shaker for 30 seconds. Covered plate and incubate at 37°C for 30 minutes. Cool the plate to room temperature then measure the absorbance at 562nm on the plate reader (VERSA max).

2.2.8 Western blot

2.2.8.1 Sample preparation

Loading buffer 4x (Bio-Rad) was added to the protein sample obtained from protein isolation, mixed well then incubated the sample for 5 minutes at 95°C, 300 rpm for more complete disruption of molecular interaction, the samples were stored in a -20C° fridge for longer storage.

2.2.8.2 Gel-electrophoresis

Mini-PROTEAN Tetra Cell system (BIO-RAD) was used during gel electrophoresis. 400mL electrophoresis buffer was poured into the electrophoresis tank, 20µg of the protein sample was loaded onto a 12% SDS polyacrylamide gel, Precision Plus Protein™ Dual Color Standards (BIO-RAD) was used as the molecular weight standards. Ran the gel with 70 volts for 40 minutes until

marker bands are visible, then ran at 120 volts for 1 hour, and keep track of the lowest band for 30 minutes.

2.2.8.3 Gel transfer/ Blot

X cell II TM Blot Module (Invitrogen) was used for gel transfer. Wet the PVDF membrane for 1 minute with methanol before equilibration in transfer buffer. Raised gels in ddH_2O and equilibrate in Blotbuffer for 15 minutes. Prepare the gel and membrane sandwich then fill it into the cassette. Filled the tank and cassette with Blotbuffer. cooling the transfer tank with ice. Gels were transferred for 2 hours onto PVDF transfer membrane (Thermo) at 35V.

2.2.8.4 Immunodetection

After transfer, wash the membrane in TBS for 5 minutes then membranes were blocked for 1 hour in blocking buffer. Wash the membrane for 5 minutes in TBS-T twice then incubate overnight at 4°C with the primary antibody which was diluted in 5% BSA. Primary antibodies used were: Rabbit anti-M3 Muscarinic Receptor Antibody (1:1000, Novus Biologicals), Rabbit anti-M4 Muscarinic Receptor Antibody (1:1000, Alomone Labs), GAPDH(D16H11) XP Rabbit mAb (1:1000, Cell Signaling), after overnight incubation, membranes were washed with TBS-T buffer 3 times, and then incubated for 1 hour at room temperature with secondary antibody: anti-rabbit IgG, HRR-linked Antibody (1:5000, Cell Signaling).

2.2.8.5 Imaging

Membranes were exposed to Clarity Max™ Western ECL Substrate (BIO-RAD) for signal detection, the image capture was performed on ChemiDoc MP Imaging System (BIO-RAD).

2.2.8.6 Result analysis

Protein bands from the western blot image were quantified by reflecting the relative amounts as a ratio of each protein band relative to the band of GAPDH control. ImageJ (FIJI) was used in the analysis. further statistical analysis was performed using the GraphPad Prism 5.

2.2.9 Measurement of cAMP levels

The cAMP analyses were performed using the HitHunter® cAMP Assay for small molecules

(DiscoverX) which is a homogeneous (no wash), gain-of-signal competitive immunoassay based on Enzyme Fragment Complementation (EFC) technology. The aim of this essay is for monitoring G-protein coupled receptor (GPCR) activation based on 3'-5'-cyclic adenosine monophosphate (cAMP) production in cells. A series of tests were performed to investigate the functional study of Gαi- coupled receptor (CHRM4), these tests contain two-part, first is the Forskolin test which is to investigate the EC80 of Forskolin, the second is the Gαi agonist challenge assay which is to figure out the Gαi- coupled receptor (CHRM4) function.

2.2.9.1 Sample preparation and assay preparation

During the cell plating, cells were seeded in white-walled 96-well tissue culture treated plate (DiscoverX) with 20,000 cells per well. The forskolin serial dilutions for the Forskolin test or Gαi agonist solution for Gαi agonist challenge assay were prepared in a separate dilution plate before adding to desired wells, see the illustration for the specific process (Figure 6).

Figure 6. The sample preparation protocol of cAMP assay.

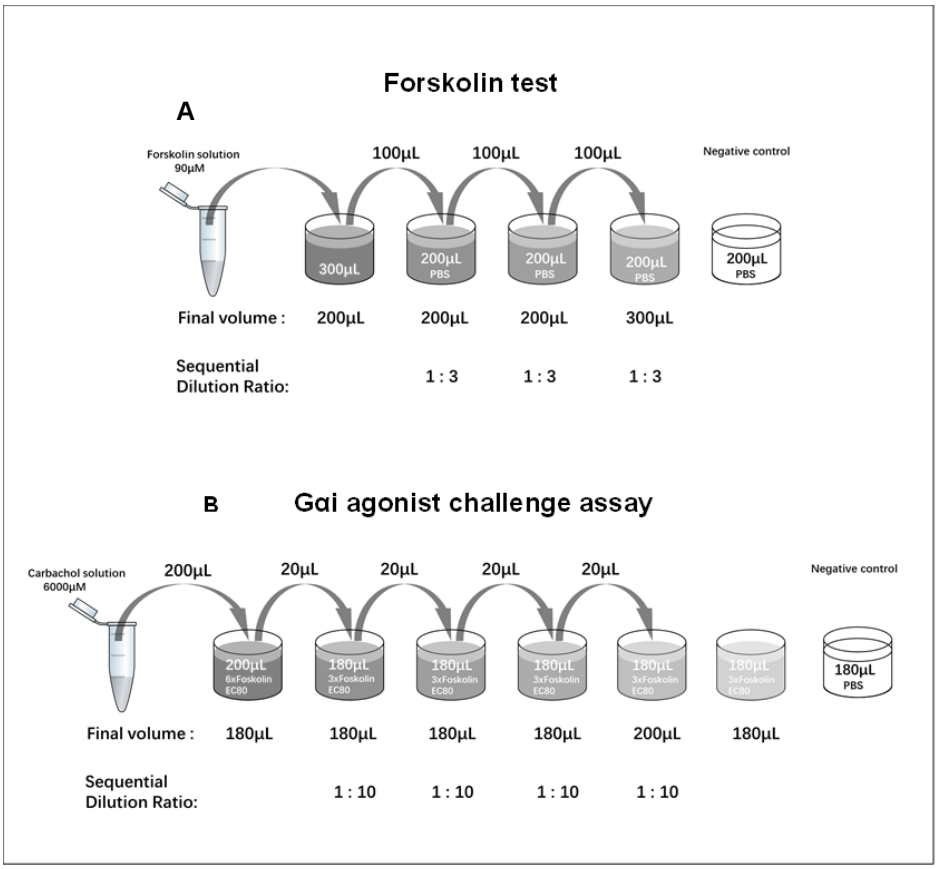

2.2.9.2 Assay protocol schematic

Detail introduction for the protocol is shown in the flow chart (Figure 7).

Figure 7. The protocol of cAMP assay.

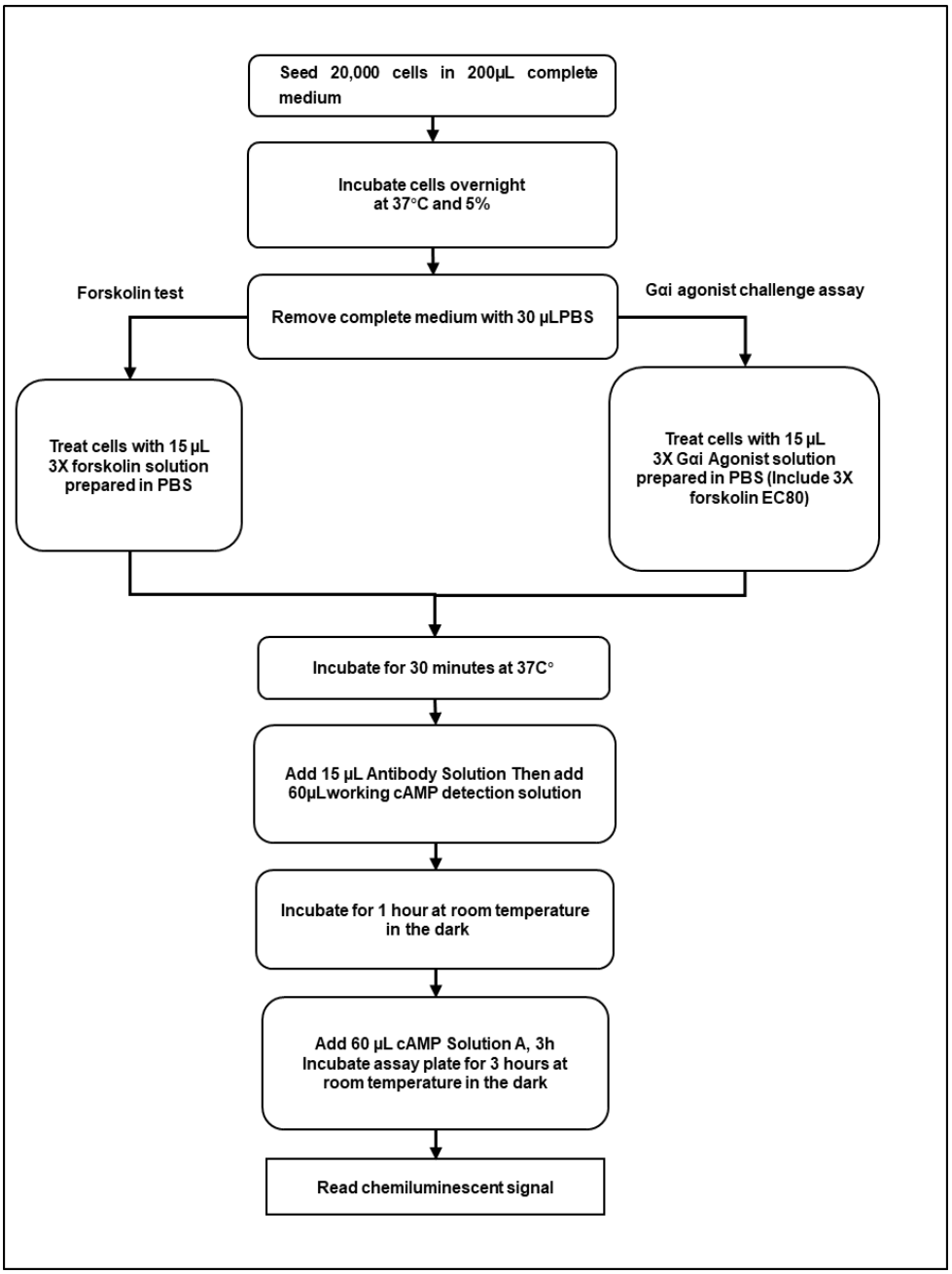

2.2.9.3 Assay Plate Reading

After the last incubation step, the plate was read using a standard luminescence plate reader (FilterMax F3). The microplate reader was set up for endpoint reading with an integration time of 0.4 seconds, the plate was dark-adapted for 1 minute before reading.

2.2.9.4 Result analysis

Results were given in relative luminescence units (RLU), the data was initially analysed using SoftMax® Pro Microplate Data Acquisition and Analysis Software (Version 6.5.1), further statistical analysis, and calculation of EC50 and EC80 was performed using the GraphPad Prism 5.

2.2.10 Fluorescence-activated cell scanning (FACS) indo-1 calcium assay

BxPc3, DanG, and Panc1 cells were subcultured in 175cm^2, cultured overnight to allow cells to attach to the plate and grow. Changed medium on next day morning and then cultured for 48 hours to allow cells to reach 70% confluence. On the assay day during sample preparation, collected 1x10^7 cells of each cell in a 15ml tube, re-suspend the cells in 1.0 ml of cell loading media (PBS containing 1mM calcium, 1mM magnesium, and 0.5% BSA.), add 2µl of Indo-1 (2mg/ml, dissolve in 20% Pluronic F-127 DMSO solution) to each sample (4µM final concentration) and incubate the cells with Indo-1 for 30 minutes at 37°C. After staining pellet cells at 400g for 5 minutes, aspirate the supernatants then resuspend the cells gently in 1ml CLM, rest cells for 15 minutes before acquiring any data. During the FACS testing, 100µl (1 x 10^6 cells total) of cell suspension was added into the FACS test tube and used for further test. UV (355 nm) laser-equipped flow cytometers (BD LSRFortessa™) were used, this dye is ratiometric and requires filter sets around 400 nm (calcium-bound) and 500 nm (calcium-free), so the filter was set for BUV395 (450/50) and BUV496 (530/30). Ratiometric changes in calcium concentration are calculated as the ratio of emission in the low wavelength filter to the emission in the high wavelength filter.

2.2.11 Fluorescence-activated cell scanning (FACS) BrdU assay

2.2.11.1 Sample preparation

PDAC cells were seeded on a 6-well plate with a density of $5x10^5$ cells/well and cultured for 24 hours with a complete medium. The following day, 10 µL of BrdU solution (1 mM BrdU in 1x DPBS) was directly added to each mL of culture medium. Left 3 wells of cells without BrdU labeling, these cells were used as the sample for BrdU FMO control (Fluorescence Minus One Control). Incubate the treated cells for 2 hours in the same condition of cell culturing. After incubation the media was aspirated, then 500µL (Versene) was added to the wells and further incubate for 10 minutes to rinse the cells. Cells were collected and washed by FACS buffer 1 time (300gx/RT/5min), then cells were counted and divided into 10^6 cells/sample acquisition tube (Falcon®), discard the supernatant after centrifuging (300gx/RT/5min).

2.2.11.2 Immunofluorescent staining of cell surface antigens

10^6 BrdU-pulsed cells were labeled with 1µL Muscarinic Acetylcholine Receptor M3/CHRM3 antibody (IgG, Novus Biologicals) primary antibody or 0.5µL of Rabbit IgG (Novus Biologicals) as an Isotype control for the primary antibody, cells were vortexed, incubated for 30 minutes at room temperature in the dark, then cells were washed with 2 ml FACS buffer (300gx/RT/5min). 0.63 µL secondary antibody Rabbit IgG APC-conjugated Antibody (Novus Biologicals) was added to the CHRM3 antibody labeled sample and the Isotype control antibody labeled sample, cells were vortexed, incubated for 30 minutes at room temperature in the dark, then cells were washed with 2 ml FACS buffer (300gx/RT/5min). The input of the antibody depends on stock concentration, the detail was shown in Table 8.

Table 8. Quantity of the primary and isotype control antibody in BrdU assay.

Antibody Name	Concentration	Input volume / sample	Input dose / sample
Muscarinic Acetylcholine Receptor M3 antibody	0.5µg/µL	1µL	0.5µg
Rabbit IgG Isotype Control	1µg/µL	0.5µL	0.5µg

2.2.11.3 Immunofluorescent staining of BrdU

The BrdU assay was performed using the BrdU Flow Kits (BD Pharmingen™), according to the manufacturer's protocol. The panel setup is shown in Table2.6. After staining of cell surface antigens, fixed and permeabilized the cells with 100 µL BD Cytofix/ Cytoperm Buffer, then incubated the cells for 30 minutes on ice, after incubation, washed the cells with 1 mL of 1x BD Perm/Wash Buffer. Resuspend the cells in 100 µL of BD Cytoperm Permeabilization Buffer Plus per tube then Incubate the cells for 10 minutes on ice. Washed the cells in 1 mL of 1x BD Perm/Wash Buffer. Resuspend the cells in 100 µL of BD Cytofix/ Cytoperm Buffer per tube, then incubate the cells for 5 minutes on ice, wash the cells in 1 mL of 1X BD Perm/Wash Buffer. Treated cells with DNase to expose incorporated BrdU by using 100 µL of diluted DNase (30 µg DNase) per tube then incubated for 1 hour at 37°C. Wash the cells n 1 mL of 1x BD Perm/Wash Buffer. Stain BrdU by incubating cells with 1µL FITC conjugated anti-BrdU antibody (contain in BrdU Flow Kits) for 20 minutes at room temperature, then washed the cells in 1 mL of 1x BD Perm/Wash Buffer. Stain total DNA for cell cycle analysis by resuspending the cells in 20 µL of the 7-AAD solution and incubating 30 minutes at room temperature. Resuspend the cells in 1 mL of FACS buffer stored at 4°C for further analysis by flow cytometry.

Table 9. BrdU assay Panel set up

Antibody Name	M3 FMO control	BrdU FMO control	M3 Isotype control	Test sample
BrdU-pulse	yes	No	yes	yes
Muscarinic Acetylcholine Receptor M3 Antibody	No	yes	No	yes
Rabbit IgG Isotype Control	No	No	yes	No
Rabbit IgG APC-conjugated Antibody	No	yes	yes	yes
Anti-BrdU antibody (FITC-conjugated)	yes	yes	yes	yes

2.2.11.4 Instrument setup

The FACS analysis was done by using FACS Fortessa (BD Biosciences). The instrument was set up in 4 steps:

- Adjusted the FSC (Forward Scatter) vs SSC (Sidewards Scatter) parameters to ensure the cell populations within the scale.
- Adjusted the PMTs (photomultiplier tubes) so that the negative populations fall around channel 10^2.
- Adjusted 7-AAD–%APC to bring the PE signal to the left.
- Adjusted APC–%7-AAD to bring the PE signal down.

For optimal resolution, acquire using a low flow rate to make sure the rate was no greater than 400 events per second.

2.2.11.5 Data analysis

BD FACSDiva™ Software v8.0 was used to collect the data and initial analyze. Further statistical analyses were performed using the GraphPad Prism 5.

2.2.12 Cell viability assay (EZ4U)

BxPc3, DanG, and Panc1 cells were seeded in the 96-well plate at the density of 2×10^3 cells/well, cultured overnight to allow cells to attach to the plate and grow. The next morning the medium was changed into 200 µl full medium (RPMI1640+10%FBS) or starvation medium (RPMI1640) together with different concentrations of the desired drug. After culturing for desired stimulation time, the medium was changed to 200µl fresh medium on the assay day and then 20 µl of the EZ4U dye substrate was added to each well before a further 3 hours incubation in 37°C. After incubation, the plate was removed from the incubator and gently mixed by tipping the plate at all four sides. The absorbance is measured by a microplate-reader (VERSA max), set at 450 nm with 620 nm as a reference.

2.2.13 Colony-forming assay

BxPc3, DanG, and Panc1 cells were seeded in the 12-well plate at the density of 5×10^3 cells/well, cultured overnight to allow cells to attach to the plate and grow. The next morning the medium was changed into 2000 µl full medium (RPMI1640+10%FBS) or starvation medium (RPMI1640) together with different concentrations of the desired drug. After culturing for desired stimulation time, the medium was changed to 2000µl fresh medium on the assay day and Colonies are fixed with glutaraldehyde (6.0% v/v), stained with crystal violet (0.5% w/v).

2.2.14 Patient's survival curve analysis

The TCGA survival curve was analyzed from the public data of the Human Protein Atlas. The patients were classified into two groups based on the FPKM target gene expression level (Fragments Per Kilobase of exon model per Million mapped fragments). The prognosis of each patients group was examined by Kaplan-Meier survival estimators, the survival outcomes were compared by log-rank tests.

2.2.15 Statistical analysis

Data analysis was performed with GraphPad Prism (ver 5.0, GraphPad Software Inc, La Jolla, CA, USA). Data were presented as the mean±SEM. Student's t-test, one-way ANOVA analyses with Bonferroni post-tests were used. A value of $p<0.05$ was considered statistically significant. ($p <0.05$ (*), $p<0.01$ (**) and $p<0.001$ (***)). The EC50 value and the Hill Slope were determined from the agonist reference curve. EC80 was calculated using an online EC80 calculator QuickCalc by GraphPad (graphpad.com/quickcalcs/Ecanything1.cfm).

3 Results

3.1 Expression of CHRMs in PDAC cell lines

As the first step, the expression of muscarinic receptors on PDAC cells was investigated. Therefore, three geno- and phenotypical different established PDAC cell lines were selected (BxPc3, DanG, and Panc1). The BxPc3 cell line has a wild-type *KRAS* gene, the other two have mutated *KRAS* alleles. The DanG and BxPc3 cell lines are epithelial phenotypes, the Panc1 cell line has a mesenchymal phenotype.

Employing RT-PCR, we detected mRNA expression of *CHRM1, CHRM3, CHRM4,* and *CHRM5* but not of *CHRM2* in all three PDAC cell lines tested (Figure 8). According to the strength of the band, the muscarinic receptor expression among these three PDAC cell lines implicated different expression levels.

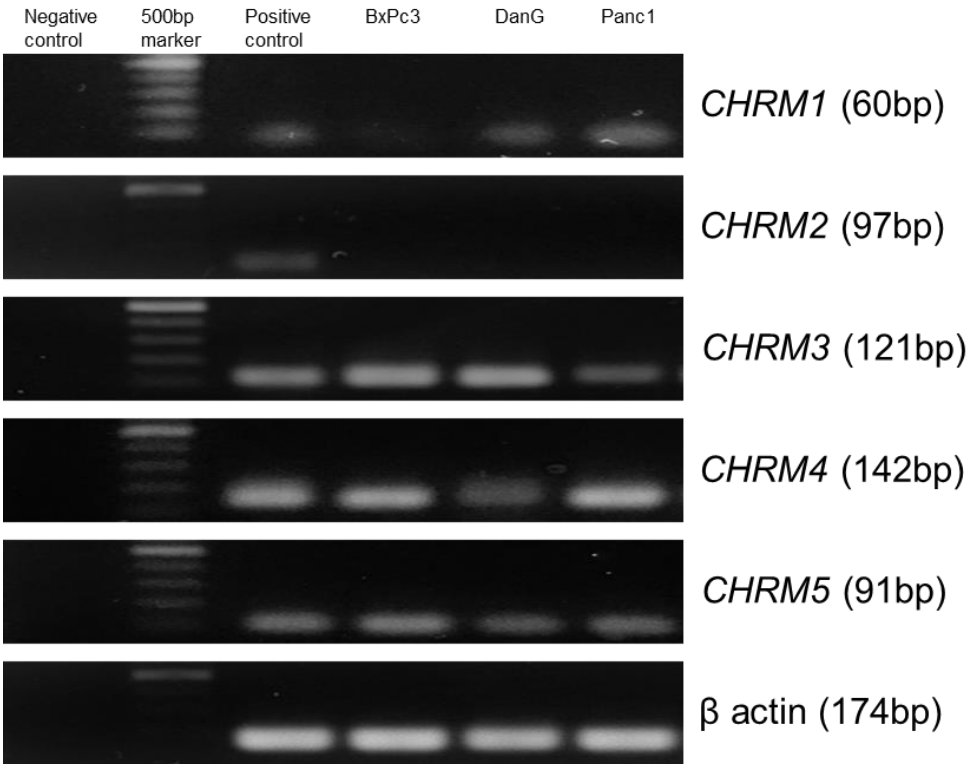

Figure 8. RT-PCR of different Muscarinic receptor subtypes in PDAC cell lines.
Panc1 and DanG cell shows a clear band of CHRM1, BxPc3 just show a very weak band of *CHRM1.CHRM3, CHRM4*, and *CHRM5* mRNA bands are detectable in all three PDAC cell lines tested.

To further evaluate the expression of these muscarinic receptors, RT- qPCR was performed. The analysis revealed the highest expression of *CHRM3* in DanG cells as well as of *CHRM4* in Panc1 cells (Table 10). Considering the phenotype of these three PDAC cell lines, the epithelial-type cells tend to express higher *CHRM3* than the mesenchymal phenotype, while the mesenchymal phenotype tends to express higher *CHRM4*. Since we have only 3 cell lines included in the study, this interpretation is limited.

The mRNA expression of *CHRM1* was low in all three cell lines analyzed (Figure 9). *CHRM1* has a very low expression level relative to the housekeeping gene *GAPDH*. However, *CHRM2* was not expressed on mRNA level in any of the cell lines investigated.

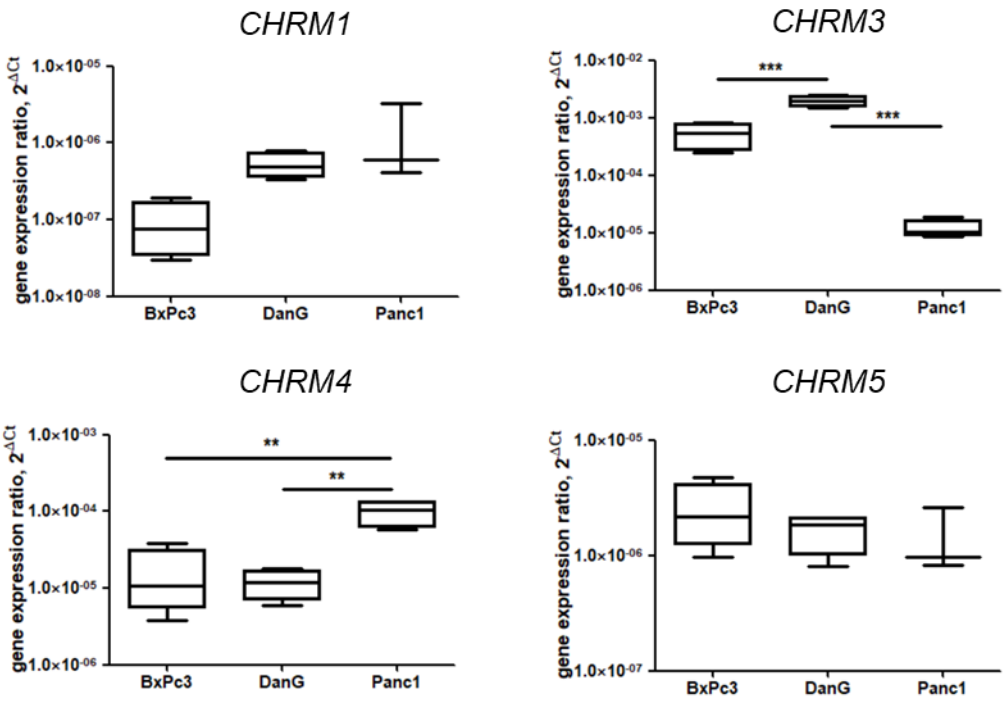

Figure 9. Real-time PCR of different Muscarinic receptor subtypes in PDAC cell lines.
CHRM1, CHRM3, CHRM4, and *CHRM5* are detectable in all the PDAC cell lines tested. Epithelial-type cells BxPc3 and DanG tend to express higher *CHRM3* than the mesenchymal phenotype Panc1. *CHRM4* shows a higher expression in the mesenchymal phenotype Panc1 cell line.

Table 10. The Muscarinic receptor expression level in PDAC cell lines.

Cell line	Phenotypes		Genotype					
	Epithe-lial	Mesenchy-mal	*KRAS*	*CHRM1*	*CHRM2*	*CHRM3*	*CHRM4*	*CHRM5*
BxPc-3	✓		Wild	Low	Negative	Middle	Middle	High
DanG	✓		G12V	Middle	Negative	High	High	Middle
Panc-1		✓	G12D	High	Negative	Low	Low	Low

Since *CHRM3* and *CHRM4* are the higher expressed subtypes of the muscarinic receptor, further experiments were focusing on these two receptor subtypes. As protein level expression is the requirement of a functional receptor, expression of these receptors on protein levels was investigated by Western blotting.

Both *CHRM3* and *CHRM4* were expressed at protein levels among all these three PDAC cell lines. The receptor expression on protein level matched the mRNA level expression result of RT-qPCR. Among the PDAC cell lines in the study, DanG cells expressed CHRM3 at a higher level while the Panc1 cells expressed the CHRM4 at a higher level, both on mRNA level and protein levels (Figure 10. A, B).

A.

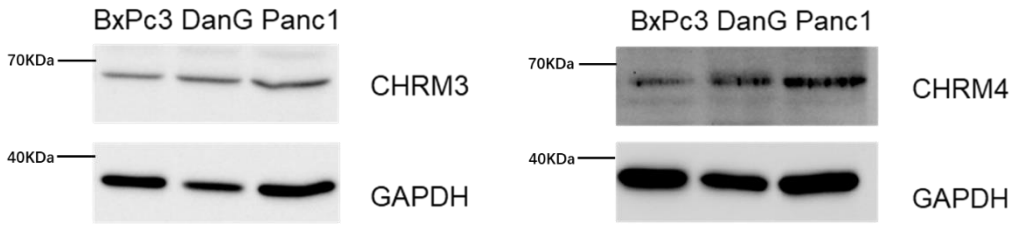

B.

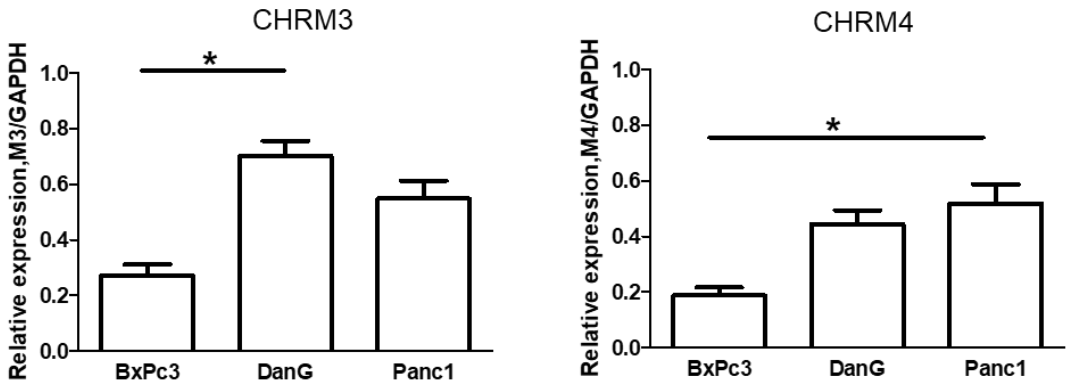

Figure 10. The protein level of CHRM3 and CHRM4 in PDAC cell lines.

Analysis of the online database of The Human Protein Atlas (www.proteinatlas.org) has given us a more macro perspective of muscarinic receptor expression among common solid tumors. According to this online database, PDAC has a distinct CHRM4 expression (Figure 11), but the expression of CHRM3 relatively low (Date not shown). This result shows in PDAC tissue, on protein level there is a higher CHRM4 expression. This differs from the result in our cell line study which shows there is a relatively higher CHRM3 expression. This different may come from the influence of cancer associated microenvironment and this topic will be further talked in the Discussion section.

Figure 11. The expression of CHRM4 in different cancers(https://www.proteinatlas.org/ENSG00000180720-CHRM4/pathology)

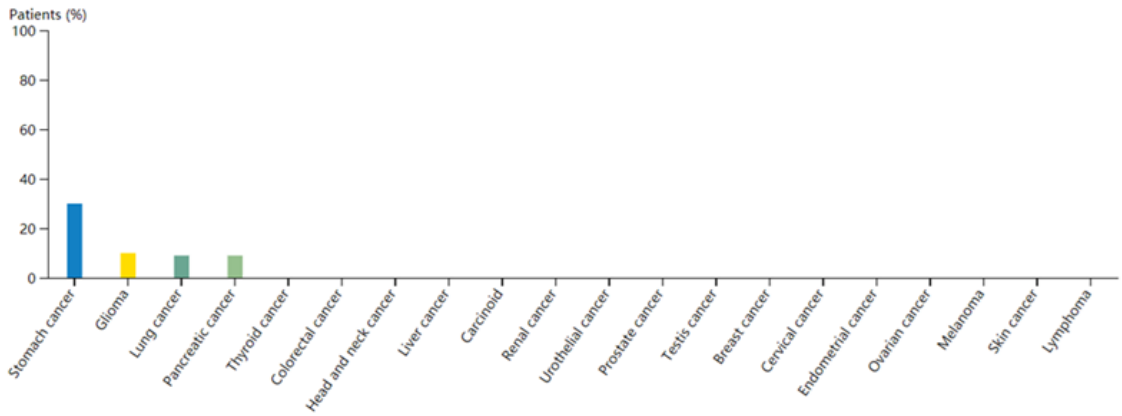

3.2 CHRM3 is functional in PDAC cells

After proving the expression of the receptor, we wanted to investigate the functionality and therefore potential biological relevance of these muscarinic receptors. We aimed to find out whether the highly expressed CHRMs are functional in PDAC cell lines investigated.

It is well known, that CHRM3 is involved in the activation of phospholipase C which leads to release of calcium from intracellular storages [60]. Therefore, we measured Ca^{2+} release after activation of CHRM3 with the unselective CHRMs-agonist carbachol. Indeed, such activation led to a significant increase in the intracellular calcium concentration in BxPc3 and DanG, but not in Panc1 cells which represent the lowest level of CHRM3 expression, and this effect can be abolished by the CHRM3 selective blocker Darifenacin (Figure 12). Based on these data, we can conclude that CHRM3 is functional in PDAC cells.

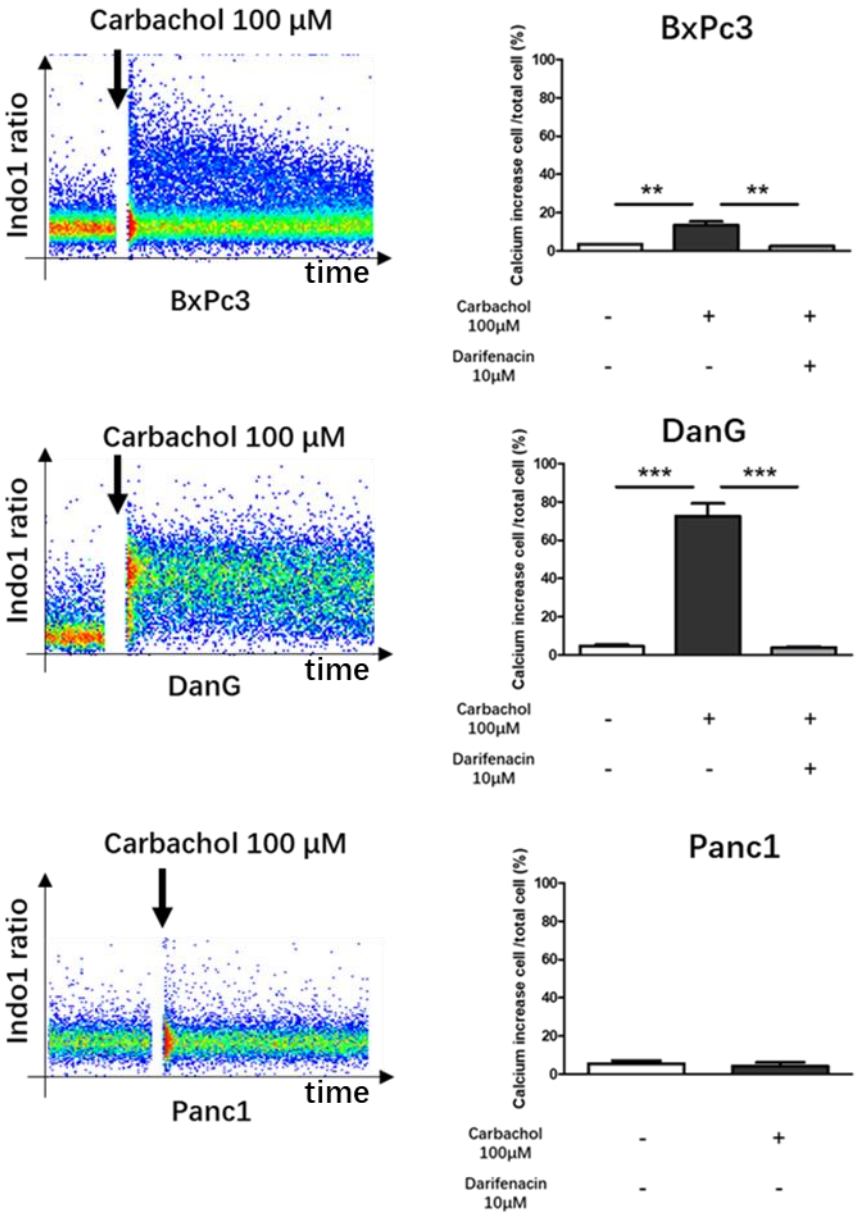

Figure 12. The CHRM3 function assay.
Most of the DanG cells can have an intracellular Ca^{2+} increase when stimulated with carbachol, only a small part of BxPc3 cells can have such a reaction. This effect is proved to act through CHRM3 since CHRM3 blocker Darifenacin can abolish the effect. Panc1 cells have no effect with carbachol treatment.

3.3 Starvation leads to the overexpression of *CHRM3* in PDAC cells

Earlier studies showed that stress conditions affect the expression of *CHRMs* [61]. The starvation culturing condition represents a stress condition the cells. There is also evidence showing that starvation leads to overexpression of *CHRM3* [62]. Therefore, we cultivated PDAC cells with

and without serum and measured their capacity to express *CHRM3*. First, we measure the cell viability of cells after starvation in comparison to normal culturing conditions. The result shows starvation is stressful for PDAC cells, the cell viability is lower after starvation, which means it challenged the cells' survival (Figure 13. A). The RT-qPCR shows this starvation condition also can lead to an up-regulation of *CHRM3* mRNA expression in PDAC cells, this result might imply that expression of *CHRM3* in PDAC could also be influenced by the nutritional conditions (Figure 13. B).

A.

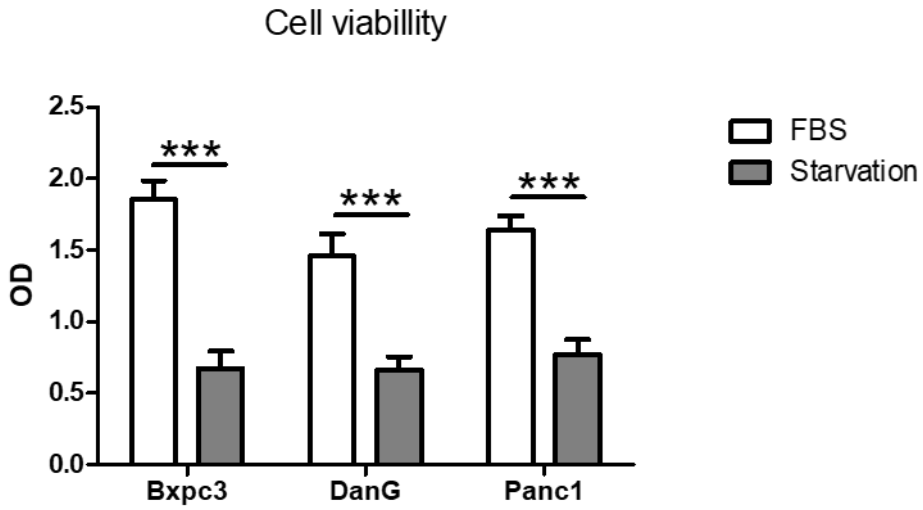

B.

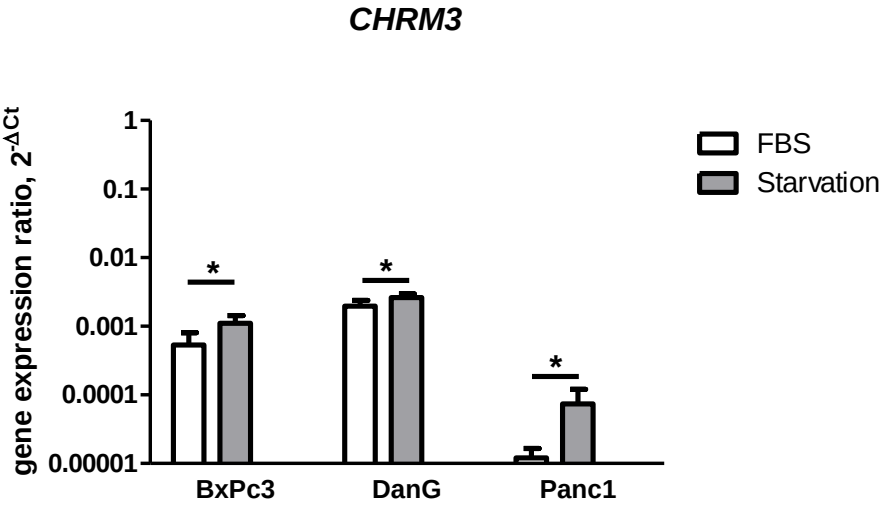

Figure 13. *CHRM3* expression in different culturing conditions.

All three PDAC cell line cells have an enhanced *CHRM3* expression during the starvation condition.

We also observed changes in the morphology of all three PDAC cell lines during starvation, the cells acquire a more spindle-like shape (Figure 13). This phenomenon is quite significant in DanG cells since it has an epithelial phenotype. Under regular culture conditions, the DanG cells are dispersed and protruded the pseudopodium (Figure 14). Some papers show that starvation can be a promoter of the EMT process. Our studies support these results morphologically although we did not further investigate EMT in our study [63,64].

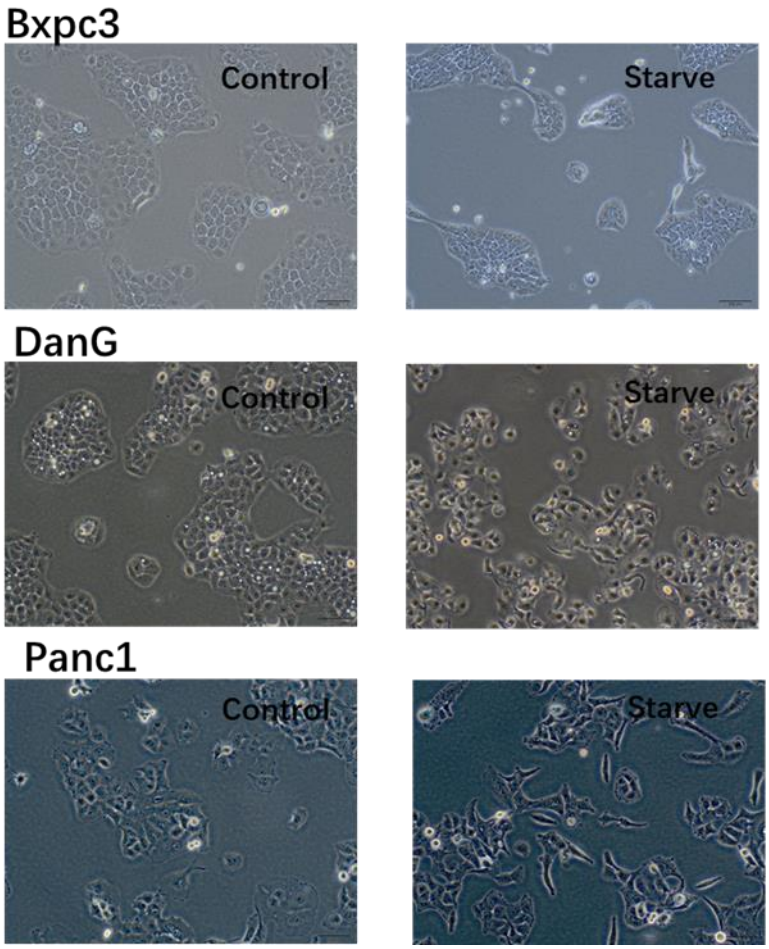

Figure 14. The morphology of PDAC cells in different culturing conditions.

3.4 The function of CHRM4 is doubtful in PDAC cells

Regarding the CHRM4, it is known that the active receptor can inhibit adenylyl cyclase and leads to a decrease of the intracellular cAMP concentration [65]. Therefore, we measured cAMP levels in our PDAC cells using the same unselective CHRMs-agonist carbachol. First, we use Forskolin as a positive control since Forskolin is a direct agonist of the adenylyl cyclase. We got a positive result in all the three PDAC cell lines with Forskolin. After calculation, the Panc1 cell line has the highest level of adenylyl cyclase since the value of EC50 is the lowest (Table 11, Figure 15).

Table 11. The EC50 and EC80 of Forskolin in cAMP assay.

cAMP assay	Bxpc3		DanG		Panc1	
	15000cells/well	20000cells/well	15000cells/well	20000cells/well	15000cells/well	20000cells/well
EC50 Hillslope	1.667	1.96	1.324	1.589	2.266	2.848
EC50	3.677μM	3.908μM	13.76μM	6.793μM	1.892μM	1.302μM
EC80 HillSlope	1.732	1.976	1.364	1.615	2.312	2.873
EC80	8.299μM	7.922μM	37.205μM	16.083μM	3.512μM	2.137μM

Figure 15. Drug dose-response curves of Forskolin in different PDAC cell lines.

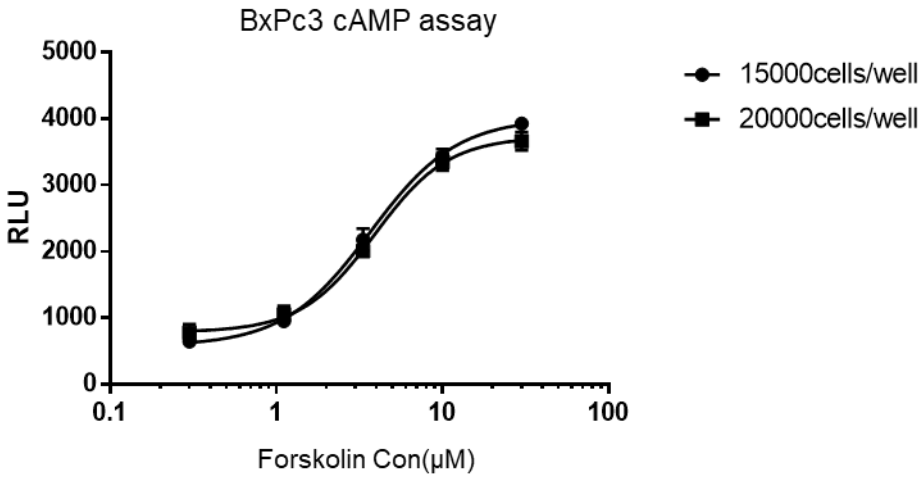

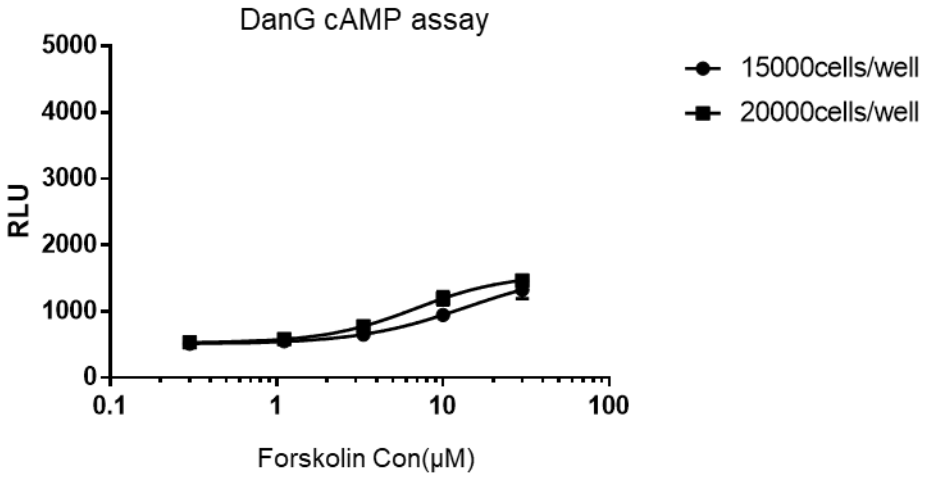

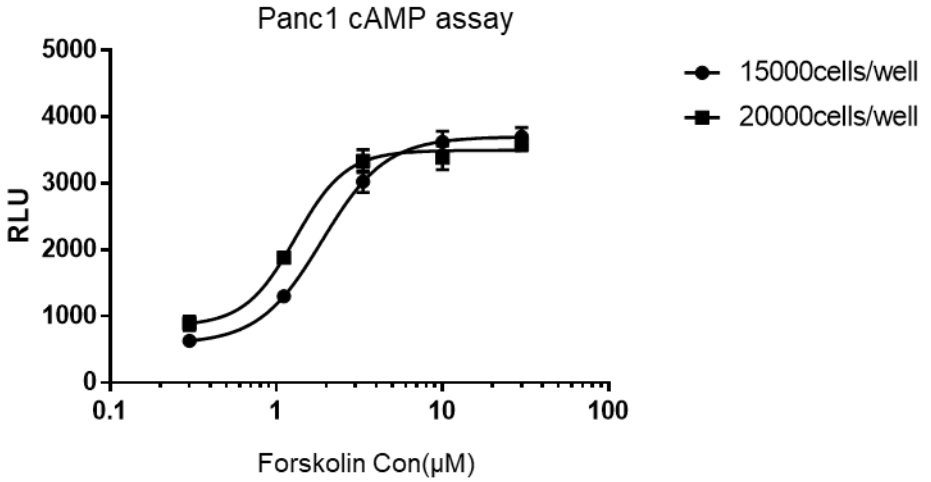

To further evaluate whether the activity of adenylyl cyclase can be modulated by activation of G proteins, the β receptor agonist Isoproterenol was used as a control. Since the β receptor is a Gs protein-coupled receptor, after activation it can increase the activity of adenylyl cyclase and lead to an intracellular cAMP increase. In this experiment Isoproterenol significantly increased the intracellular cAMP level in both the BxPc3 and Panc1 cell. This means that the intracellular cAMP level can be modulated by G protein-coupled receptors in PDAC cells (Figure 16). In contrast, carbachol did not influence the basic cellular cAMP level (Figure 16). This result led to the conclusion that the CHRM4 in PDAC cell lines may be unfunctional or does not signal through the classic cAMP pathway.

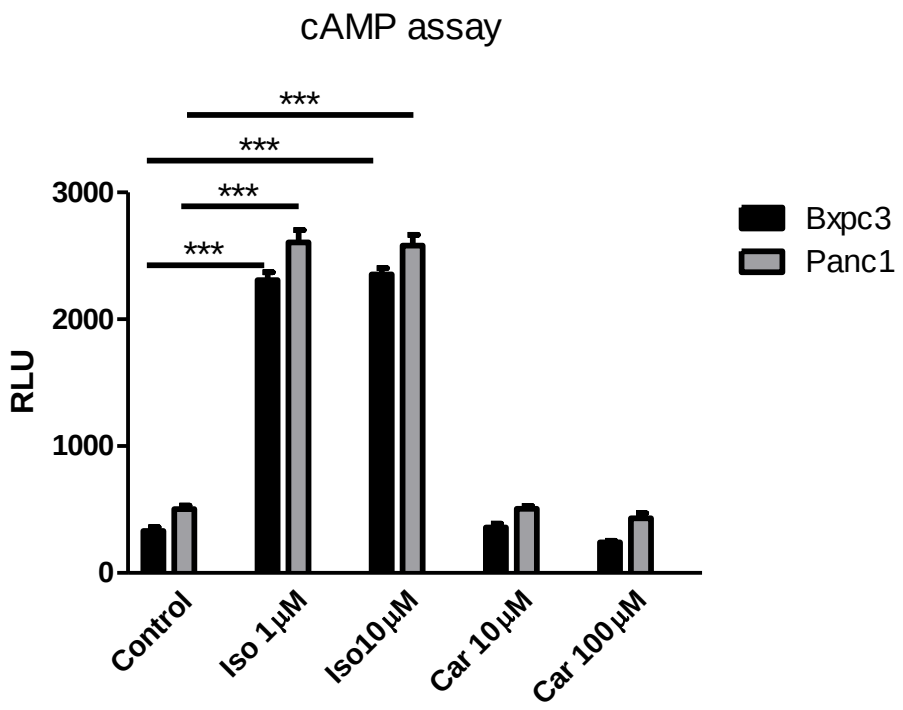

Figure 16. The level of basic cellular cAMP level changes after β receptor and muscarinic receptor activation.
Both BxPc3 and Panc1 cells can be activated by β receptor agonist Isoproterenol but not muscarinic receptor agonist carbachol.

3.5 *CHRM3* expression level correlates with PDAC patient's survival

As we had detected a functional expression of CHRM3 in PDAC, we wondered whether the expression of the *CHRM3* gene has a link to the survival of patients with PDAC. To understand this, we analyzed the publicly available data from the Human Protein Atlas (https://www.protein-atlas.org/) using TCGA RNA samples from 176 PDAC patients. We found that patients with a higher *CHRM3* expression showed a trend to a better 5-year survival (Figure 17).

Figure 17. The 5-year survival rate between *CHRM3* high and low expression (https://www.proteinatlas.org/ENSG00000133019-CHRM3/pathology/pancreatic+cancer)

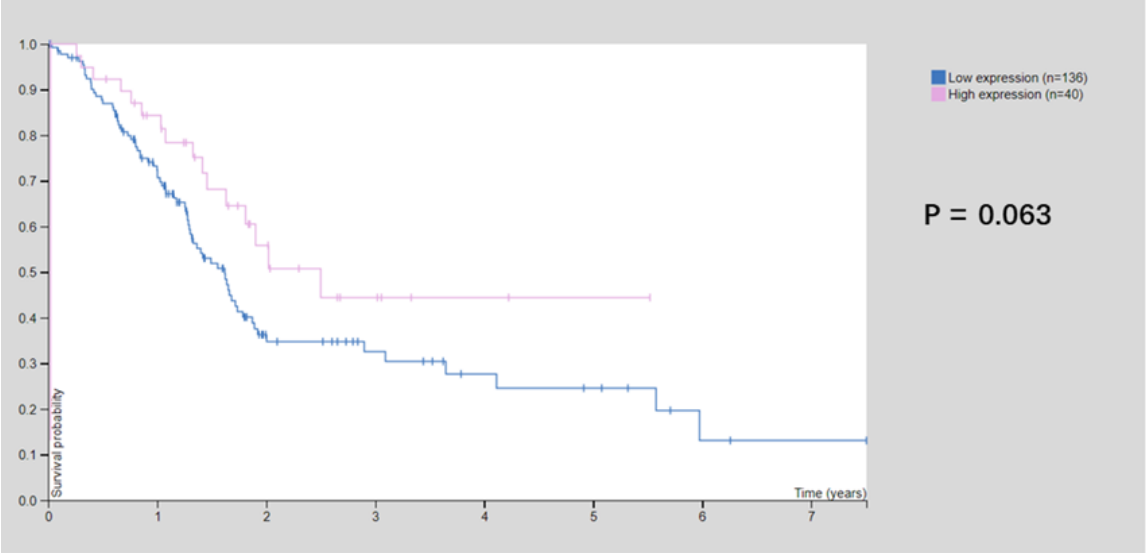

To become a first hint for understanding this survival benefit, we performed flow cytometric cell cycle analysis combined with measurement of CHRM3 expression (Figure 18). Here we found that 5.1% of the cells express CHRM3.

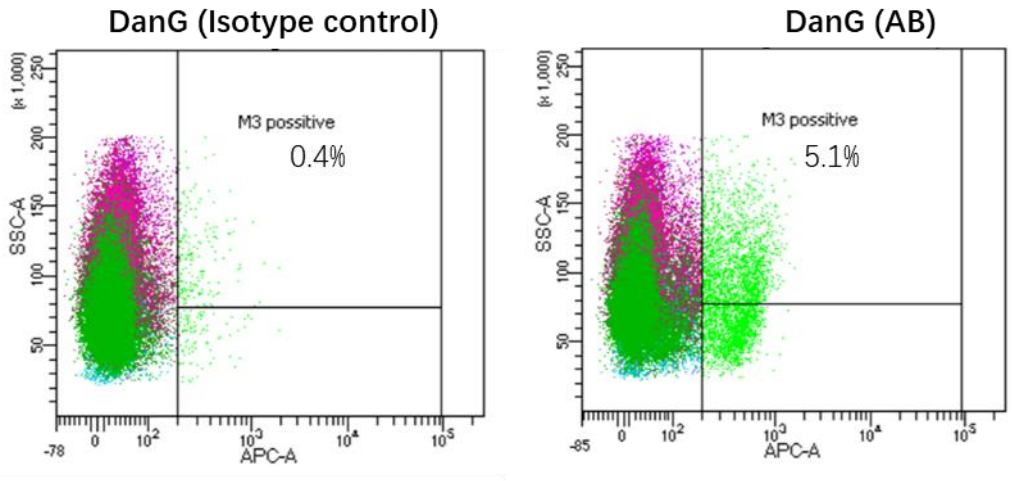

Figure 18. The CHRM3 positive subgroup cells in the DanG cell line.

For the DanG cell line, the cell cycle analysis shows over half of the cells are in the S stage (Figure 19).

DanG cell line

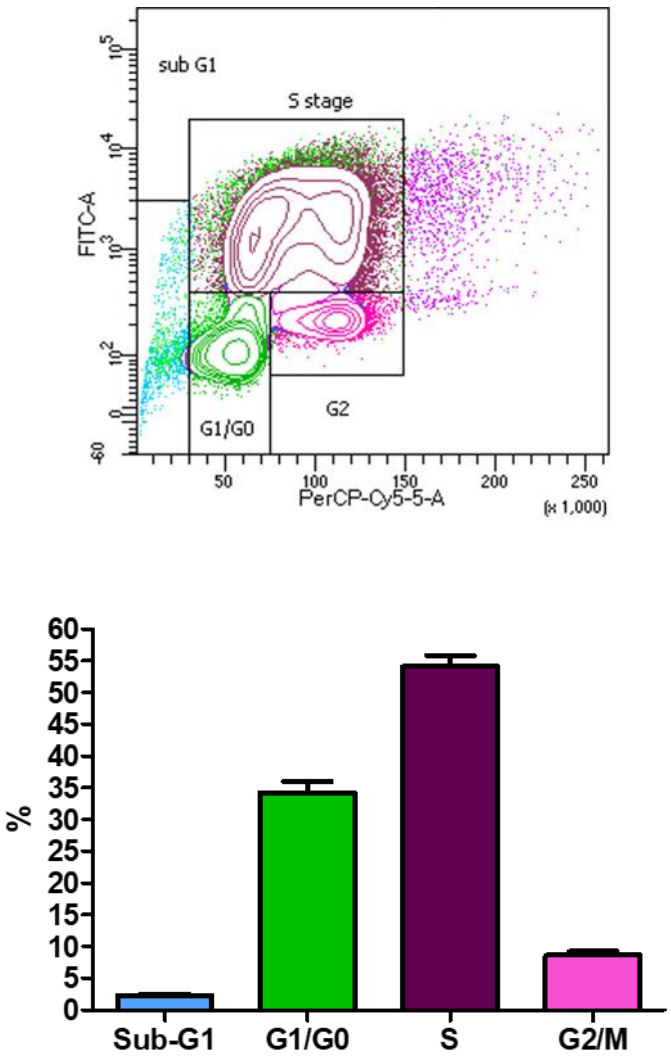

Figure 19. Cell cycle distribution of DanG cell line.

Intriguingly, we found the CHRM3 positive cells exist in all these four different cell cycle stages, which means the expression of the CHRM3 has no relation with the cell cycle check-point (Figure 20). However, the highest surface expression of CHRM3 on the cells is in the sub-G1phase which represents early apoptotic cells. Therefore, we suggest that the trend for a bet-ter survival of PDAC patients with higher CHRM3 expression could be partially due to the higher amount of apoptotic tumor cells (Figure 20).

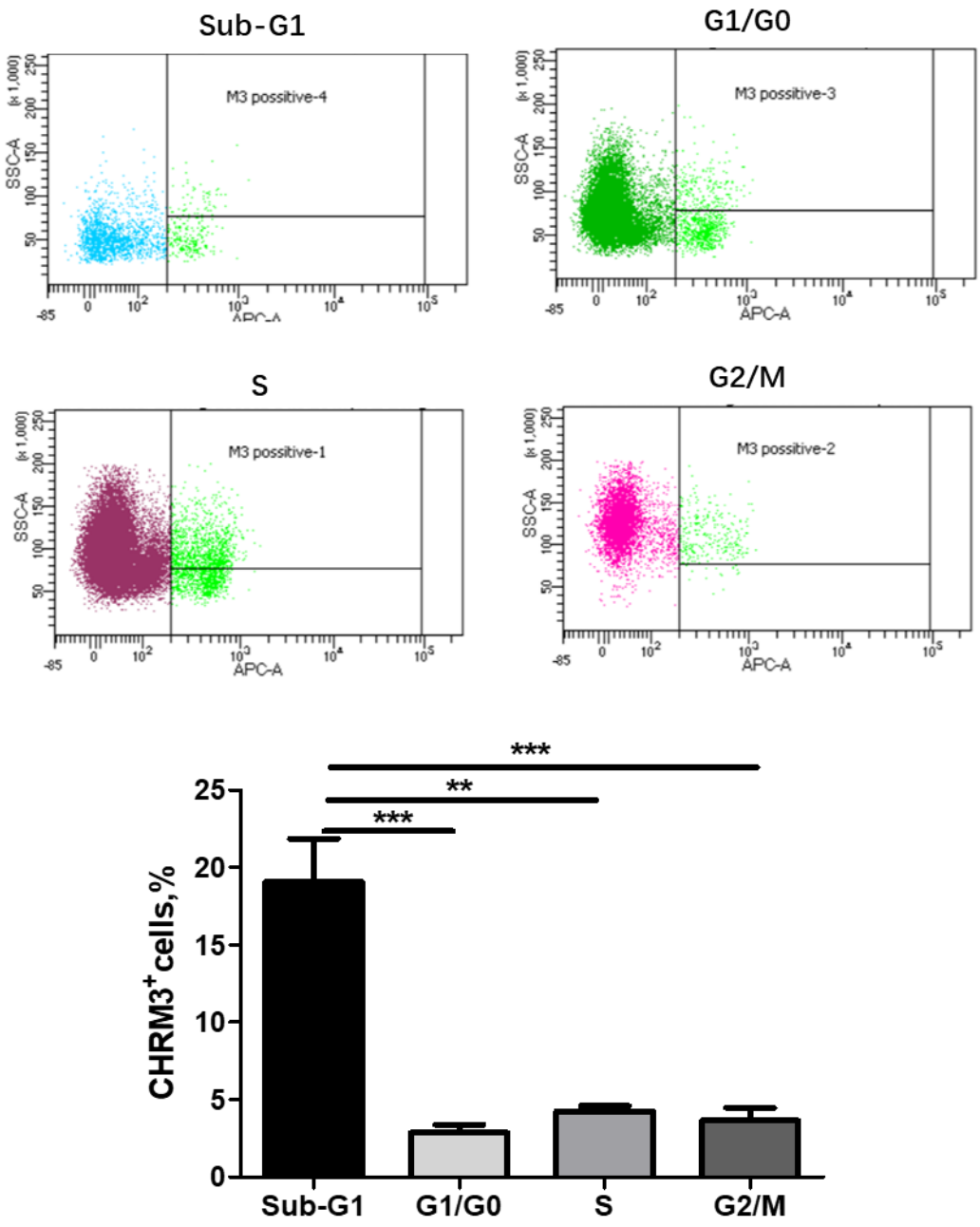

Figure 20. Cell cycle distribution of CHRM3 positive DanG cells.
In the DanG cell line, the Sub-G1 cell cycle stage has the highest percentage of CHRM3 positive cells.

The last question was whether CHRM3 is only an epiphenomenal marker of a better patient survival as well as of the sub-G1phase of cell cycle or whether CHRM3 is involved as a functional receptor in the PDAC pathogenesis. To investigate this point, we treated the PDAC cells with different concentrations of carbachol and investigated the colony formation. This treatment did not lead to differences in the treatment group (Figure 21). The absence of phenotypical effects of CHRM3 activation could be explained by the low expression of CHRM3 on the surface of PDAC

cells. To prove or disprove this assumption, we measured cell viability after the treatment in the starvation condition which leads to the overexpression of CHRM3. Also in this condition, we saw carbachol does not affect cell viability (Figure 22).

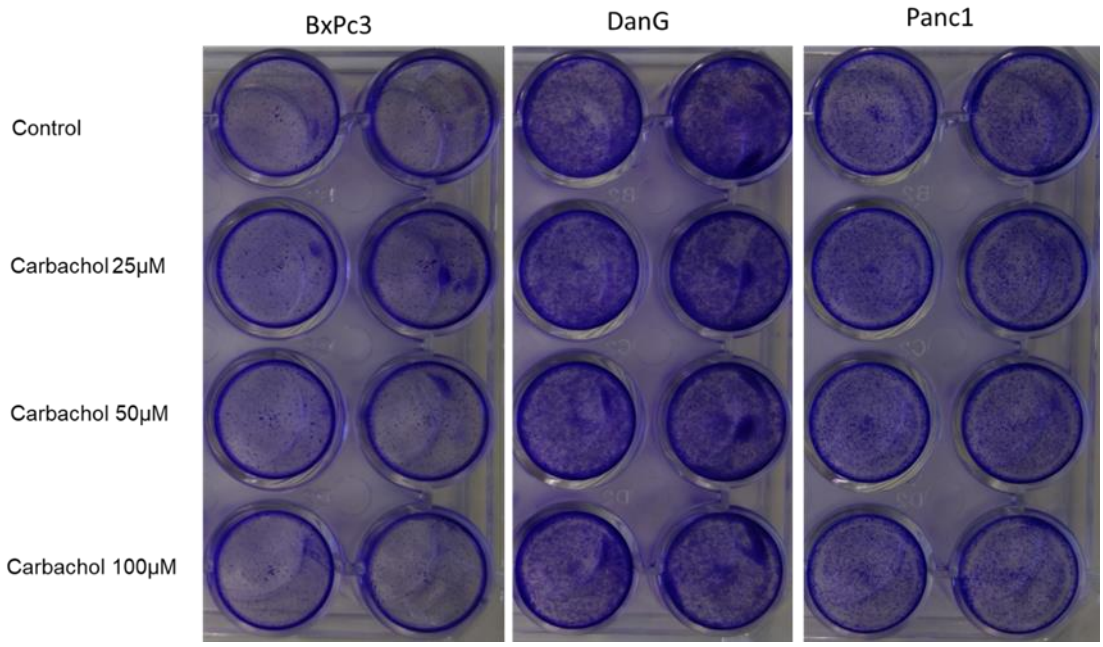

Figure 21. Colony-forming assay of PDAC cell line treated with muscarinic receptor agonist carbachol

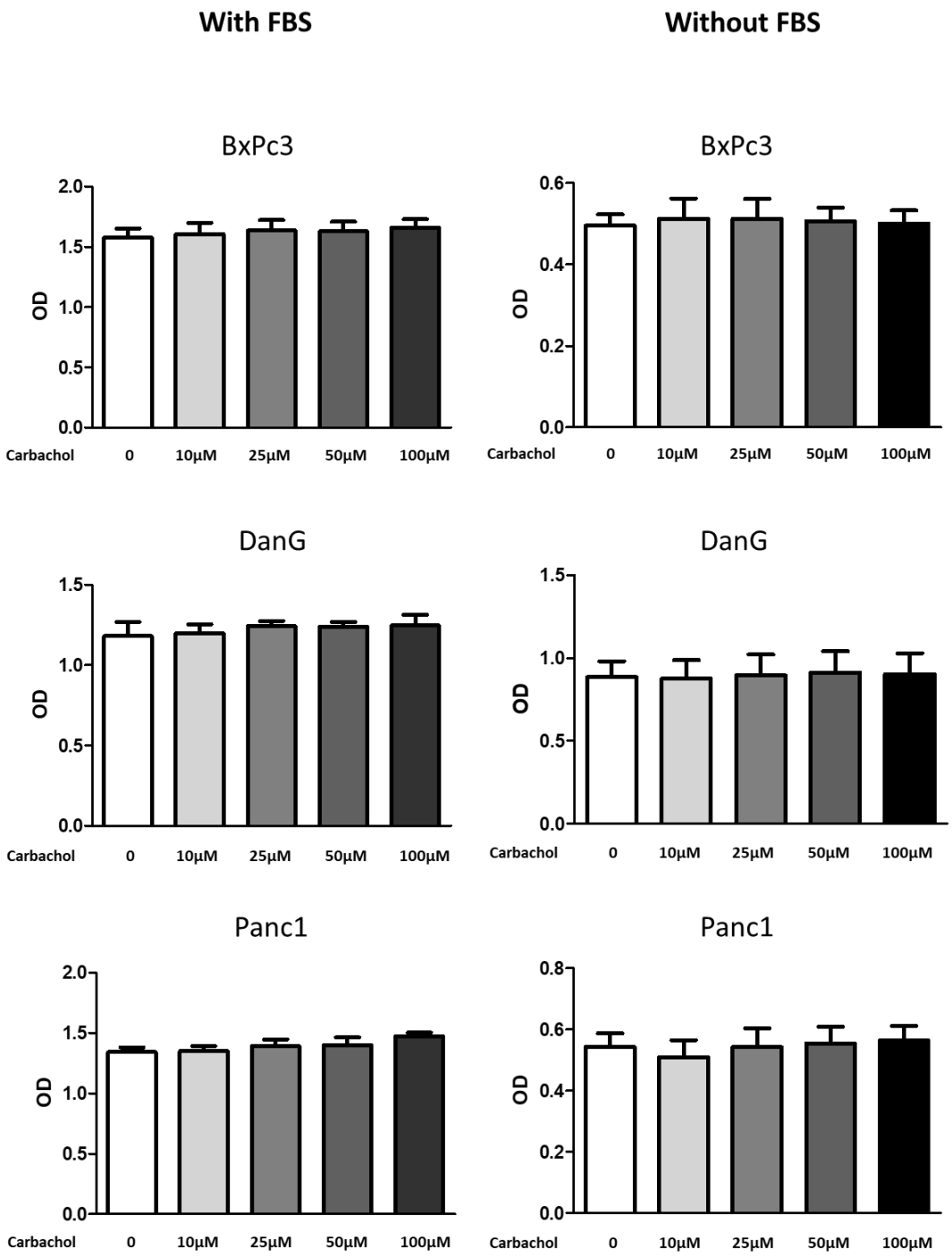

Figure 22. EZ4U cell viability assay in PDAC cell line with muscarinic receptor agonist carbachol treatment.

To further investigate the effect of the muscarinic receptor CHRM3, a selected CHRM3 antagonist Darifenacin was used. The colony formation assay shows that the survival of all the three

PDAC cell lines can be inhibited by Darifenacin with or without the no FBS starving stress condition (Figure 23).

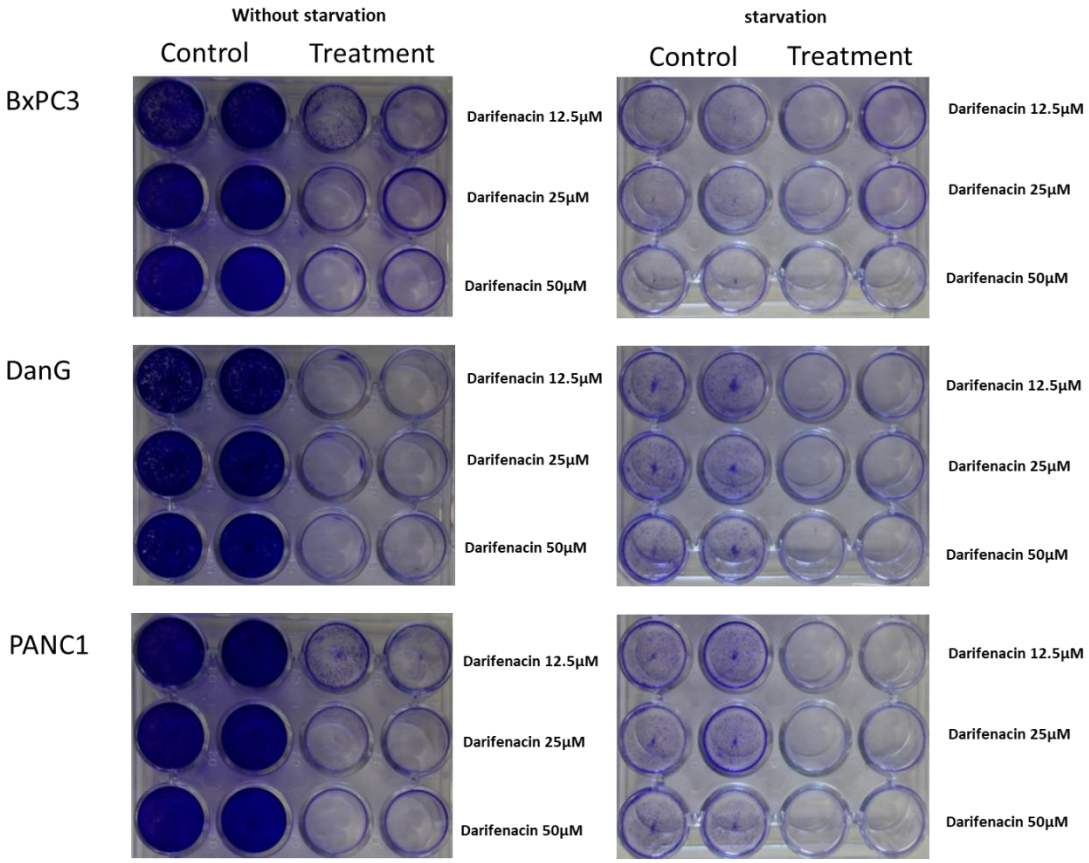

Figure 23. Colony-forming assay of PDAC cell line treated with CHRM3 blocker Darifenacin.

The cell viability assay also supports this inhibitory effect as 20μM Darifenacin can significantly inhibit the cell viability of all these PDAC cell lines, with or without starvation (Figure 24).

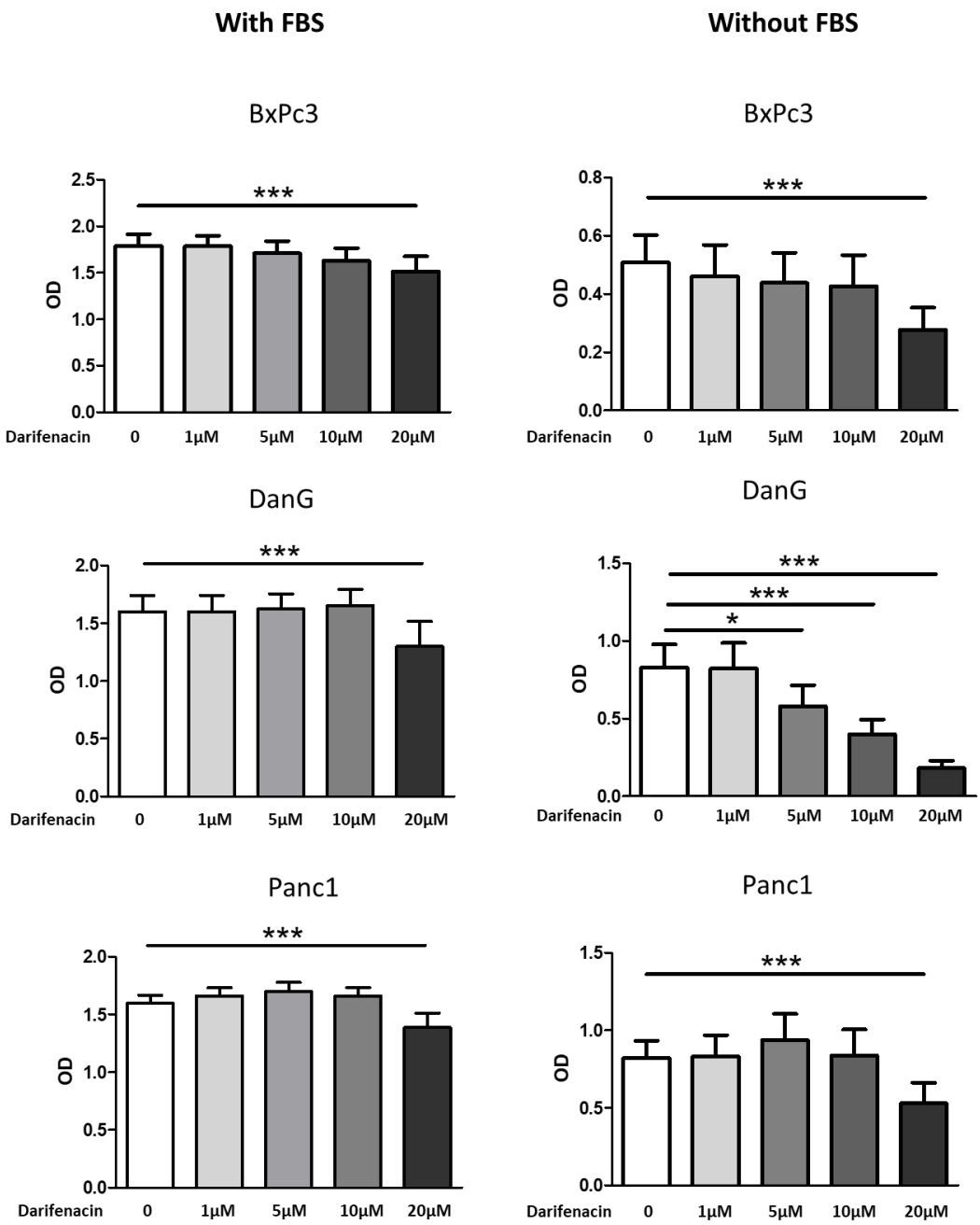

Figure 24. EZ4U cell viability assay in PDAC cell line with CHRM3 blocker Darifenacin.

However, in a further cell viability assay, we found that the carbachol pretreatment cannot abolish the inhibitory effect of Darifenacin, this means that decrease in cell viability may not be caused by the effect of the muscarinic receptor CHRM3(Figure 25).

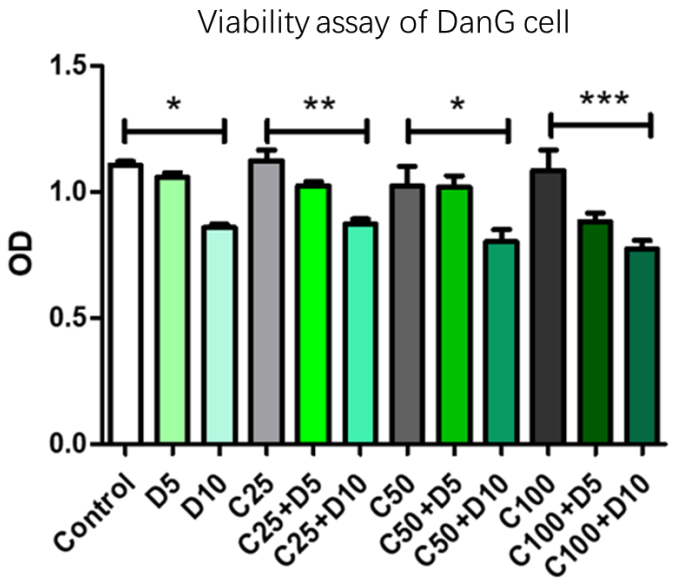

Figure 25. Cell viability assay of DanG with CHRM3 selective blocker Darifenacin.
Darifenacin treatment decreases DanG cell viability, but this effect cannot be abolished by pre-treated with muscarinic receptor agonist carbachol.

Thus, we can suggest that the activation (i.e., function) of CHRM3 on the cancer cell may be not be involved in the pathogenicity of PDAC cells.

4 Discussion

4.1 Expression of muscarinic receptor subtypes in PDAC cell lines

Early studies demonstrated the existence of different subtypes of muscarinic receptors in the endocrine and exocrine pancreas compartment [66,67]. The expression of the cholinergic receptor M3 (CHRM3) was detected in the acinar compartment and the receptor activation induces an increase of intracellular Ca^{2+} [68]. In this study, we focused on CHRM3 expression in PDAC. We showed the expression of different muscarinic receptor subtypes in human PDAC cells lines and found higher and functional relevant expression of the CHRM3 subtype. Furthermore, different PDAC cell phenotypes seem to express varying muscarinic receptor subtypes and expression levels. Our data suggest that the phenotypically more epithelial PDAC cell lines Bxpc3 and DanG have a higher CHRM3 protein expression level while pancreatic cancer cell lines with a more mesenchymal phenotype like Panc1 have a higher CHRM4 expression level.

CHRM3 has been proven to be expressed on human pancreatic acinar cells. These cells change their phenotype rapidly when cultured after isolation, losing their neurohumoral responsiveness after prolonged culture. However, there is no study investigating the changes of CHRM3 expression during the phenotypic alterations.

CHRM3 plays an important role in pancreatic exocrine secretion. It is not known whether CHRM3 is functional in PDAC. An inactivation of CHRM3 has been reported in human submandibular gland cancer. It has been shown that CHRM3 only functioned in a normal human submandibular gland duct cell line, while dysfunctional in a human submandibular carcinoma cell line and a salivary gland adenocarcinoma cell line [69]. In our study, CHRM3 did not show a function on cell viability, although the receptor activation can induce an increase of intracellular Ca^{2+} in Bxpc3 and DanG. It is tempting to speculate that CHRM3 plays also a role in the control of autocrine or paracrine signaling of PDAC cells. However, we did not study the secretion effects of CHRM3 of PDAC cell lines, this should be investigated in further studies.

As mentioned above, PDAC originates from the acinar cell compartment. Epithelial to mesenchymal transition (EMT) is believed to be the first step in PDAC carcinogenesis, this raises the possibility of a dynamic expression of the muscarinic receptor during EMT. Furthermore, it is not known whether muscarinic signaling plays a role in this process in PDAC. In other cancer entities, muscarinic receptors have been proven to be involved in this EMT process. In a cholangiocarcinoma study, CHRM3 was proved involved in the EMT process modulated via the AKT signaling pathway[70]. In our study, under normal culture conditions, DanG cells showed morphological changes. These cells are losing tight connection and become dispersed and protruded the pseudopodium during starvation. Besides this, after starvation, the expression of CHRM3 was increased. We speculate that CHRM3 may play a role during the EMT process. Investigation of CHRM3 expression during EMT could shed light on the role of CHRM3 in EMT in PDAC.

4.2 CHRM3 labeling identifies a distinct PDAC subgroup

According to our calcium flux experiments, more than 60% of DanG cells can be activated by the treatment with muscarinic receptor agonist carbachol. This effect was abolished when cells were pretreated with the CHRM3 selective blocker Darifenacin. Intriguingly, the flow cytometry revealed that only a small group of DanG cells (around 5%) expressed the CHRM3 on the cell membrane. There are several potential explanations: First of all, it could be a methodical limitation. The CHRM3 is a member of the G protein-coupled receptor family and it is known that the receptor expression is very dynamic and quite sensitive to environmental changes. If there is an active internalization, the antibody labeling efficiency during flow cytometry analysis might be affected and this may lead to undetected receptor expression. However, the internalization of CHRM3 does not abolish the receptor activation. In this regard, an earlier study showed that even the intracellular muscarinic receptor can be activated by the agonist, and can also induce an increase of intracellular calcium concentration after activation [71]. Therefore, the internalized receptors would contribute to the calcium flux experiment, while not detected in the flow cytometry analysis. Besides this, the muscarinic receptors, as G-protein-coupled receptors, have the ability for dimerization with multiple other receptors. This dimer can also be activated and in this way induce activation of downstream pathways. This means even if a cell only expresses a low level

of muscarinic receptor, the agonist still can activate the receptor and the activation effect even will be intensified by receptor dimers, this could cause an underestimation of the CHRM3 positive cell group [72,73].

Based on our results only a subgroup of DanG cells expresses CHRM3. Therefore, CHRM3 might label a distinct PDAC cell population. Further studies are needed to characterize this distinct cell population in more detail.

4.3 Activation of the muscarinic receptors in PDAC

In our study, *CHRM3*, *CHRM4*, CHRM3, and CHRM4 were detected in all three PDAC cell lines as the qPCR and western blot results showed. However, we did not find a functional role of muscarinic receptors in our calcium flux experiments in Panc1 cells. In contrast, BxPc3 and DanG show CHRM3 activity by the calcium flux assay. We did not detect a significant cAMP decrease by the cAMP assay, which represents a functional test of CHRM4 after treatment with carbachol. The reason for this could be the multiplicity of the downstream signal induced after muscarinic receptor activation.

The downstream pathway of CHRM3 is variable, the level of PLC-β, DAG, PKC can also increase as a reaction after activation of CHRM3 [74]. For the CHRM4 receptor, the decrease of the intracellular cAMP level is also the classic but not the only reactive signal. Some other ion channels, phosphodiesterase, phospholipases can also respond to the activation of CHRM4 [74]. Other potentially activatable pathways need to be investigated in further experiments.

The classic second messenger after CHRM4 activation is cAMP. cAMP plays an important role in the carcinogenesis of many cancers type including PDAC [75,76]. In the study of human pancreatic cell line (HPAC), different subtypes of adenylyl cyclase (AC) have been found[75]. In our test, AC function was tested by the AC agonist Forskolin and the beta receptor agonist Isoproterenol treatment. Forskolin and Isoproterenol can both successfully induce a rapid increase of intracellular cAMP among all three PDAC cell lines. This result support early studies which showed the existence of an active cAMP system in PDAC cells lines [77]. However, in our further experiments, stimulation of the CHRM4, as a Gαs coupled receptor and an indirect AC inhibiter, could not change the basic cAMP level in PDAC cell lines that have a positive CHRM4 expression.

This study shows in PDAC there is a high frequency of mutations in genes encoding the G proteins, especially the *GNAS* gene which is the genes encoding the G proteins Gαs[78]. Therefore, a non-functional mutation of the *CHRM4* could be considered as an explanation. It has been reported that a *CHRM5* mutation can increase the constitutive activity of the receptor and also increase the potency of carbachol in both binding and functional assays[79]. A mutation Gαs coupled receptor may have an enhancement or suppression of receptor function, in some cases even a change of activated signal pathway after stimulation. In addition, we found more DanG cells expressing intracellular CHRM3, although the labeling condition is without any agonist treatment. This uncommon location of the receptor may also have a relation with receptor mutation. According to an early study using Chinese Hamster Ovary cells (CHO cells), the mutation-induced phosphorylation-deficient CHRM3 will have deficiency during receptor internalization and arrestin recruitment[80]. In our study, we did not involve the genotype description of *CHRM3* and *CHRM4*. In further experiments, this should be studied in detail. More information about the genotype of *CHRM3* and *CHRM4* in PDAC will bring us new perspectives on the potential function of CHRM3 and CHRM4.

4.4 CHRM expression level is associated with cell viability state

In earlier studies, which have investigated muscarinic receptor function in different cancer entities, activation had been shown to modulate cell viability. However, unlike the published results in other cancer types, activation of the CHRM3 by the muscarinic agonist carbachol caused a significant change in viability in none of the human PDAC cell lines in our hands. This was even evident under serum starvation conditions, in which the CHRM3 receptor expression was shown to be higher expressed. Nevertheless, our studies have several limitations. Studies in the past have shown that the effect of muscarinic receptor CHRM3 activation varies on cell types and the particular muscarinic receptor agonist [81]. For example, activation of the CHRM3 by pilocarpine as a non-selective muscarinic receptor agonist, lead to a markedly different pattern of calcium signaling compared with carbachol in rat pancreatic acinar cells[82]. Not only calcium signaling but also other pathways like the ERK pathway may be affected by the agonist type[83]. In our

experiments, we chose carbachol since it is an unselective agonist for all the muscarinic receptor subtypes. However, under physiological conditions or in the PDAC microenvironment, the muscarinic receptor is activated by acetylcholine and bile acid. To further clarify the effect of CHRM3 on PDAC cells, we are planning to use genetically engineered mouse models which conditionally overexpress or do not express CHRM3 in murine PDAC.

Among the studies in which CHRM3 affects proliferation, the effect was proved to be calcium signaling dependent [46,84]. The effect was abolished by pretreating the cells with an intracellular Ca^{2+} chelator or a reduction of extracellular Ca^{2+} by EDTA [84]. CHRM3 activation can induce cell death and inhibit proliferation in cells that have high Rac1 activity. This effect is induced by activation of Gq/11, PLC, and PKC [85]. In our experiments, carbachol treatment leads to an increase of intracellular calcium in Bxpc3 and DanG cell lines. These two PDAC cell lines also tend to have a high Rac1 activity compared to primary pancreatic ductal cells [86]. After considering all this back information, the negative result in our cell viability assay led to one possible hypothesis that a high level and activity of cellular Rac1 might not be sufficient for transducing the muscarinic receptor signaling on proliferation in this setting.

High *CHRM3* expression was associated with a trend for better overall survival in the publicly available database and might be a potential biomarker. On the other hand, the number of PDAC cell lines we used in our study is limited. Other PDAC cell lines as T3M-4 and SU.86.86 were used in a recent study that also investigated cholinergic signals in PDAC. According to their results, carbachol can decrease cell viability in these two cell lines[4]. As the muscarinic receptor expression levels were not tested in this study, it seems possible that the carbachol effect was mediated via the nicotinic receptor as carbachol stimulates both muscarinic and nicotinic receptors even with a lower affinity for nicotinic receptors.

Nutritional deficiencies culturing conditions lead to an increase of *CHRM3* expression in our hands. However, under such stress conditions, CHRM3 activation with carbachol still cannot induce a significant effect on cell viability. This result further clarifies that cell fate determination is independent of the CHRM3 effect *in vitro* monolayer cultured PDAC cells.

The fact that the subG1 population of DanG cells has a higher percentage of CHRM3^{+} cells may also bring us to the hypothesis that CHRM3 will increase when the cells undergo an unhealthy state. This receptor may not promote a cell to undergo an apoptotic process, but provides resistance to the harsh environment. There are studies show CHRM3 receptors can be involved in cell metabolism and autophagy [87–89]. There exists the potential that the function of CHRM3 is the regulation of cell metabolism or autophagy in PDAC. For a deeper understanding of the function of CHRM3 on these cells, we need to enrich high CHRM3 expressing cells in autophagy and other cell metabolism models. Single-cell sequencing can also bring us a better understanding of the feature of this high CHRM3 expressing cell subgroup.

4.5 *CHRM3* expression level has the potential to be a prognostic marker in PDAC

After analysis of the ATCC online database, *CHRM3* mRNA expression level has the potential to be a prognostic indicator in human PDAC. This result is different from studies about *CHRM3* in other cancer types, in which patients with a higher *CHRM3* expression have shorter overall survival. The PDAC tissue has a high level of muscarinic receptor expression. According to the tissue database, CHRM3 is widely expressed in pancreatic cancer PDAC biopsy samples, 78.1% of these samples show a CHRM3 positive expression [51]. However, to evaluate the CHRM3 positive component in such an ingredient diversity PDAC tissue is difficult. Since 50-80% of PDAC tumor is stromal tissue, also other cell types in the tumor microenvironment likely express CHRM3 [90]. Evidence shows that stromal cells like pancreatic satellite cells, immune cells, and nerve fibers in PDAC tissue can express CHRM3[91,92]. As a target receptor of acetylcholine, CHRM3 also plays a role in neuronal tissue. A more elaborated immunohistochemical tissue analysis is needed to identify the expression alterations of CHRM3 during pancreatic carcinogenesis thereby clarifying the role of CHRM3 as a prognostic marker or monitoring treatment parameter.

5 Outlook

1, Further prospective studies are needed to investigate the role of *CHRM3* as a prognostic marker in PDAC. With bioinformatic analysis using the online PDAC database, the biomarker value of *CHMR3* can be evaluated among different subtypes of pancreatic cancer. To avoid potential interference of the *CHRM3* expression in the exocrine pancreas in PDAC, tissue microarray can more focus on the CHRM3 receptor expression in PDAC tissue and provide more convincing evidence.

2, Gene editing studies targeting muscarinic receptors which include knockdown and overexpression in the PDAC cell line and a genetically engineered mouse model can help clarify the interaction of muscarinic receptors and PDAC.

References

[1] Quante, A.S., Ming, C., Rottmann, M., Engel, J., Boeck, S., Heinemann, V., et al. (2016) Projections of cancer incidence and cancer‐related deaths in Germany by 2020 and 2030. *Cancer Medicine*. **5**. 2649–2656.

[2] Bray, F., Ferlay, J., Soerjomataram, I., Siegel, R.L., Torre, L.A., and Jemal, A. (2018) Global cancer statistics 2018: GLOBOCAN estimates of incidence and mortality worldwide for 36 cancers in 185 countries. *CA: A Cancer Journal for Clinicians*. **68**. 394–424.

[3] Kalser, M.H., Barkin, J., and MacIntyre, J.M. (1985) Pancreatic cancer. Assessment of prognosis by clinical presentation. *Cancer*. **56**. 397–402.

[4] Pfitzinger, P.L., Fangmann, L., Wang, K., Demir, E., Gürlevik, E., Fleischmann-Mundt, B., et al. (2020) Indirect cholinergic activation slows down pancreatic cancer growth and tumor-associated inflammation. *Journal of Experimental & Clinical Cancer Research : CR*. **39**. 289.

[5] Sahin, I.H., Iacobuzio-Donahue, C.A., and O'Reilly, E.M. (2016) Molecular signature of pancreatic adenocarcinoma: an insight from genotype to phenotype and challenges for targeted therapy. *Expert Opinion on Therapeutic Targets*. **20**. 341–359.

[6] Hruban, R.H., Goggins, M., Parsons, J., and Kern, S.E. (2000) Progression model for pancreatic cancer. *Clinical Cancer Research : An Official Journal of the American Association for Cancer Research*. **6**. 2969–2972.

[7] Schwartz, A.M. and Henson, D.E. (2007) Familial and sporadic pancreatic carcinoma, epidemiologic concordance. *The American Journal of Surgical Pathology*. **31**. 645–646.

[8] Hruban, R.H., Adsay, N. V, Albores-Saavedra, J., Compton, C., Garrett, E.S., Goodman, S.N., et al. (2001) Pancreatic intraepithelial neoplasia: a new nomenclature and classification system for pancreatic duct lesions. *The American Journal of Surgical Pathology*. **25**. 579–586.

[9] Houbracken, I., de Waele, E., Lardon, J., Ling, Z., Heimberg, H., Rooman, I., et al. (2011) Lineage tracing evidence for transdifferentiation of acinar to duct cells and plasticity of human pancreas. *Gastroenterology*. **141**. 731–41, 741.e1–4.

[10] Liou, G.-Y., Döppler, H., Necela, B., Krishna, M., Crawford, H.C., Raimondo, M., et al. (2013) Macrophage-secreted cytokines drive pancreatic acinar-to-ductal metaplasia through NF-κB and MMPs. *The Journal of Cell Biology*. **202**. 563–577.

[11] Liou, G.-Y., Döppler, H., DelGiorno, K.E., Zhang, L., Leitges, M., Crawford, H.C., et al. (2016) Mutant KRas-Induced Mitochondrial Oxidative Stress in Acinar Cells Upregulates EGFR Signaling to Drive Formation of Pancreatic Precancerous Lesions. *Cell Reports*. **14**. 2325–2336.

[12] Ardito, C.M., Grüner, B.M., Takeuchi, K.K., Lubeseder-Martellato, C., Teichmann, N., Mazur, P.K., et al. (2012) EGF receptor is required for KRAS-induced pancreatic tumorigenesis. *Cancer Cell*. **22**. 304–317.

[13] Guerra, C., Collado, M., Navas, C., Schuhmacher, A.J., Hernández-Porras, I., Cañamero, M., et al. (2011) Pancreatitis-induced inflammation contributes to pancreatic cancer by inhibiting oncogene-induced senescence. *Cancer Cell*. **19**. 728–739.

[14] Aichler, M., Seiler, C., Tost, M., Siveke, J., Mazur, P.K., Da Silva-Buttkus, P., et al. (2012) Origin of pancreatic ductal adenocarcinoma from atypical flat lesions: a comparative study in transgenic mice and human tissues. *The Journal of Pathology*. **226**. 723–734.

[15] Furukawa, T., Klöppel, G., Volkan Adsay, N., Albores-Saavedra, J., Fukushima, N., Horii, A., et al. (2005) Classification of types of intraductal papillary-mucinous neoplasm of the pancreas: a consensus study. *Virchows Archiv : An International Journal of Pathology*. **447**. 794–799.

[16] Strobel, O., Rosow, D.E., Rakhlin, E.Y., Lauwers, G.Y., Trainor, A.G., Alsina, J., et al. (2010) Pancreatic duct glands are distinct ductal compartments that react to chronic injury and mediate Shh-induced metaplasia. *Gastroenterology*. **138**. 1166–1177.

[17] Storz, P. (2017) Acinar cell plasticity and development of pancreatic ductal adenocarcinoma. *Nature Reviews. Gastroenterology & Hepatology*. **14**. 296–304.

[18] Mitchem, J.B., Hamilton, N., Gao, F., Hawkins, W.G., Linehan, D.C., and Strasberg, S.M. (2012) Long-term results of resection of adenocarcinoma of the body and tail of the pancreas using radical antegrade modular pancreatosplenectomy procedure. *Journal of the American College of Surgeons*. **214**. 46–52.

[19] Pedrazzoli, S. (2015) Extent of lymphadenectomy to associate with pancreaticoduodenectomy in patients with pancreatic head cancer for better tumor staging. *Cancer Treatment Reviews*. **41**. 577–587.

[20] Delpero, J.R., Jeune, F., Bachellier, P., Regenet, N., Le Treut, Y.P., Paye, F., et al. (2017) Prognostic Value of Resection Margin Involvement After Pancreaticoduodenectomy for Ductal Adenocarcinoma: Updates From a French Prospective Multicenter Study. *Annals of Surgery*. **266**. 787–796.

[21] Ghaneh, P., Kleeff, J., Halloran, C.M., Raraty, M., Jackson, R., Melling, J., et al. (2019) The Impact of Positive Resection Margins on Survival and Recurrence Following Resection and Adjuvant Chemotherapy for Pancreatic Ductal Adenocarcinoma. *Annals of Surgery*. **269**. 520–529.

[22] Manji, G.A., Olive, K.P., Saenger, Y.M., and Oberstein, P. (2017) Current and Emerging Therapies in Metastatic Pancreatic Cancer. *Clinical Cancer Research : An Official Journal of the American Association for Cancer Research*. **23**. 1670–1678.

[23] Schloithe, A.C., Sutherland, K., Woods, C.M., Blackshaw, L.A., Davison, J.S., Toouli, J., et al. (2008) A novel preparation to study rat pancreatic spinal and vagal mechanosensitive afferents in vitro. *Neurogastroenterology and Motility : The Official Journal of the European Gastrointestinal Motility Society*. **20**. 1060–1069.

[24] Love, J.A., Yi, E., and Smith, T.G. (2007) Autonomic pathways regulating pancreatic exocrine secretion. *Autonomic Neuroscience : Basic & Clinical*. **133**. 19–34.

[25] Klein, E., Salinas, A., Shemesh, E., and Dreiling, D.A. (1988) Effects of autonomic denervation on canine exocrine pancreatic secretion and blood flow. *International Journal of Pancreatology : Official Journal of the International Association of Pancreatology*. **3**. 165–170.

[26] Buijs, R.M., Chun, S.J., Niijima, A., Romijn, H.J., and Nagai, K. (2001) Parasympathetic and sympathetic control of the pancreas: a role for the suprachiasmatic nucleus and other hypothalamic centers that are involved in the regulation of food intake. *The Journal of Comparative Neurology*. **431**. 405–423.

[27] Rodriguez-Diaz, R., Speier, S., Molano, R.D., Formoso, A., Gans, I., Abdulreda, M.H., et al. (2012) Noninvasive in vivo model demonstrating the effects of autonomic innervation on pancreatic islet function. *Proceedings of the National Academy of Sciences of the United States of America*. **109**. 21456–21461.

[28] Ceyhan, G.O., Bergmann, F., Kadihasanoglu, M., Altintas, B., Demir, I.E., Hinz, U., et al. (2009) Pancreatic neuropathy and neuropathic pain--a comprehensive pathomorphological study of 546 cases. *Gastroenterology*. **136**. 177-186.e1.

[29] Nakao, A., Harada, A., Nonami, T., Kaneko, T., and Takagi, H. (1996) Clinical significance of carcinoma invasion of the extrapancreatic nerve plexus in pancreatic cancer. *Pancreas*. **12**. 357–361.

[30] Liang, D., Shi, S., Xu, J., Zhang, B., Qin, Y., Ji, S., et al. (2016) New insights into perineural invasion of pancreatic cancer: More than pain. *Biochimica et Biophysica Acta*. **1865**. 111–122.

[31] Shimada, K., Nara, S., Esaki, M., Sakamoto, Y., Kosuge, T., and Hiraoka, N. (2011) Intrapancreatic nerve invasion as a predictor for recurrence after

pancreaticoduodenectomy in patients with invasive ductal carcinoma of the pancreas. *Pancreas*. **40**. 464–468.

[32] Schorn, S., Demir, I.E., Haller, B., Scheufele, F., Reyes, C.M., Tieftrunk, E., et al. (2017) The influence of neural invasion on survival and tumor recurrence in pancreatic ductal adenocarcinoma - A systematic review and meta-analysis. *Surgical Oncology*. **26**. 105–115.

[33] Zhao, C.-M., Hayakawa, Y., Kodama, Y., Muthupalani, S., Westphalen, C.B., Andersen, G.T., et al. (2014) Denervation suppresses gastric tumorigenesis. *Science Translational Medicine*. **6**. 250ra115.

[34] Liebig, C., Ayala, G., Wilks, J., Verstovsek, G., Liu, H., Agarwal, N., et al. (2009) Perineural invasion is an independent predictor of outcome in colorectal cancer. *Journal of Clinical Oncology : Official Journal of the American Society of Clinical Oncology*. **27**. 5131–5137.

[35] Renz, B.W., Takahashi, R., Tanaka, T., Macchini, M., Hayakawa, Y., Dantes, Z., et al. (2018) β2 Adrenergic-Neurotrophin Feedforward Loop Promotes Pancreatic Cancer. *Cancer Cell*. **33**. 75-90.e7.

[36] Renz, B.W., Tanaka, T., Sunagawa, M., Takahashi, R., Jiang, Z., Macchini, M., et al. (2018) Cholinergic Signaling via Muscarinic Receptors Directly and Indirectly Suppresses Pancreatic Tumorigenesis and Cancer Stemness. *Cancer Discovery*. **8**. 1458–1473.

[37] Saloman, J.L., Albers, K.M., Li, D., Hartman, D.J., Crawford, H.C., Muha, E.A., et al. (2016) Ablation of sensory neurons in a genetic model of pancreatic ductal adenocarcinoma slows initiation and progression of cancer. *Proceedings of the National Academy of Sciences of the United States of America*. **113**. 3078–3083.

[38] Jurcak, N.R., Rucki, A.A., Muth, S., Thompson, E., Sharma, R., Ding, D., et al. (2019) Axon Guidance Molecules Promote Perineural Invasion and Metastasis of Orthotopic Pancreatic Tumors in Mice. *Gastroenterology*. **157**. 838-850.e6.

[39] Dai, H., Li, R., Wheeler, T., Ozen, M., Ittmann, M., Anderson, M., et al. (2007) Enhanced survival in perineural invasion of pancreatic cancer: an in vitro approach. *Human Pathology*. **38**. 299–307.

[40] Hayakawa, Y., Sakitani, K., Konishi, M., Asfaha, S., Niikura, R., Tomita, H., et al. (2017) Nerve Growth Factor Promotes Gastric Tumorigenesis through Aberrant Cholinergic Signaling. *Cancer Cell*. **31**. 21–34.

[41] Liebl, F., Demir, I.E., Rosenberg, R., Boldis, A., Yildiz, E., Kujundzic, K., et al. (2013) The severity of neural invasion is associated with shortened survival in colon cancer. *Clinical Cancer Research : An Official Journal of the American Association for Cancer Research*. **19**. 50–61.

[42] Albo, D., Akay, C.L., Marshall, C.L., Wilks, J.A., Verstovsek, G., Liu, H., et al. (2011) Neurogenesis in colorectal cancer is a marker of aggressive tumor behavior and poor outcomes. *Cancer*. **117**. 4834–4845.

[43] Dubeykovskaya, Z., Si, Y., Chen, X., Worthley, D.L., Renz, B.W., Urbanska, A.M., et al. (2016) Neural innervation stimulates splenic TFF2 to arrest myeloid cell expansion and cancer. *Nature Communications*. **7**. 10517.

[44] Magnon, C., Hall, S.J., Lin, J., Xue, X., Gerber, L., Freedland, S.J., et al. (2013) Autonomic nerve development contributes to prostate cancer progression. *Science (New York, N.Y.)*. **341**. 1236361.

[45] Kruse, A.C., Kobilka, B.K., Gautam, D., Sexton, P.M., Christopoulos, A., and Wess, J. (2014) Muscarinic acetylcholine receptors: novel opportunities for drug development. *Nature Reviews. Drug Discovery*. **13**. 549–560.

[46] Wang, N., Yao, M., Xu, J., Quan, Y., Zhang, K., Yang, R., et al. (2015) Autocrine Activation of CHRM3 Promotes Prostate Cancer Growth and Castration Resistance via

CaM/CaMKK-Mediated Phosphorylation of Akt. *Clinical Cancer Research : An Official Journal of the American Association for Cancer Research*. **21**. 4676–4685.

[47] Williams, C.L. and Lennon, V.A. (1991) Activation of muscarinic acetylcholine receptors inhibits cell cycle progression of small cell lung carcinoma. *Cell Regulation*. **2**. 373–381.

[48] Lei, Y., Hamada, Y., Li, J., Cong, L., Wang, N., Li, Y., et al. (2016) Targeted tumor delivery and controlled release of neuronal drugs with ferritin nanoparticles to regulate pancreatic cancer progression. *Journal of Controlled Release : Official Journal of the Controlled Release Society*. **232**. 131–142.

[49] Sailer, M., Oppitz, M., and Drews, U. (2000) Induction of cellular contractions in the human melanoma cell line SK-mel 28 after muscarinic cholinergic stimulation. *Anatomy and Embryology*. **201**. 27–37.

[50] Frucht, H., Jensen, R.T., Dexter, D., Yang, W.L., and Xiao, Y. (1999) Human colon cancer cell proliferation mediated by the M3 muscarinic cholinergic receptor. *Clinical Cancer Research : An Official Journal of the American Association for Cancer Research*. **5**. 2532–2539.

[51] Song, P., Sekhon, H.S., Lu, A., Arredondo, J., Sauer, D., Gravett, C., et al. (2007) M3 muscarinic receptor antagonists inhibit small cell lung carcinoma growth and mitogen-activated protein kinase phosphorylation induced by acetylcholine secretion. *Cancer Research*. **67**. 3936–3944.

[52] Español, A.J., Salem, A., Di Bari, M., Cristofaro, I., Sanchez, Y., Tata, A.M., et al. (2020) The metronomic combination of paclitaxel with cholinergic agonists inhibits triple negative breast tumor progression. Participation of M2 receptor subtype. *PloS One*. **15**. e0226450.

[53] Jiménez, E. and Montiel, M. (2005) Activation of MAP kinase by muscarinic cholinergic receptors induces cell proliferation and protein synthesis in human breast cancer cells. *Journal of Cellular Physiology*. **204**. 678–686.

[54] Rimmaudo, L.E., de la Torre, E., Sacerdote de Lustig, E., and Sales, M.E. (2005) Muscarinic receptors are involved in LMM3 tumor cells proliferation and angiogenesis. *Biochemical and Biophysical Research Communications*. **334**. 1359–1364.

[55] Guizzetti, M., Costa, P., Peters, J., and Costa, L.G. (1996) Acetylcholine as a mitogen: muscarinic receptor-mediated proliferation of rat astrocytes and human astrocytoma cells. *European Journal of Pharmacology*. **297**. 265–273.

[56] Gray-Schopfer, V., Wellbrock, C., and Marais, R. (2007) Melanoma biology and new targeted therapy. *Nature*. **445**. 851–857.

[57] Ferretti, M., Fabbiano, C., Di Bari, M., Ponti, D., Calogero, A., and Tata, A.M. (2012) M2 muscarinic receptors inhibit cell proliferation in human glioblastoma cell lines. *Life Sciences*. **91**. 1134–1137.

[58] Lucianò, A.M., Perciballi, E., Fiore, M., Del Bufalo, D., and Tata, A.M. (2020) The Combination of the M2 Muscarinic Receptor Agonist and Chemotherapy Affects Drug Resistance in Neuroblastoma Cells. *International Journal of Molecular Sciences*. **21**. 1–16.

[59] Guizzetti, M., Wei, M., and Costa, L.G. (1998) The role of protein kinase C alpha and epsilon isozymes in DNA synthesis induced by muscarinic receptors in a glial cell line. *European Journal of Pharmacology*. **359**. 223–233.

[60] Caulfield, M.P. (1993) Muscarinic receptors--characterization, coupling and function. *Pharmacology & Therapeutics*. **58**. 319–379.

[61] Myslivecek, J. and Kvetnanský, R. (2006) The effects of stress on muscarinic receptors. Heterologous receptor regulation: yes or no? *Autonomic & Autacoid Pharmacology*. **26**. 235–251.

[62] Lin, K., Wang, D., and Sadée, W. (2002) Serum response factor activation by muscarinic receptors via RhoA. Novel pathway specific to M1 subtype involving

calmodulin, calcineurin, and Pyk2. *The Journal of Biological Chemistry*. **277**. 40789–40798.

[63] Lee, S.-H., Jung, Y.-S., Chung, J.-Y., Oh, A.Y., Lee, S.-J., Choi, D.H., et al. (2011) Novel tumor suppressive function of Smad4 in serum starvation-induced cell death through PAK1-PUMA pathway. *Cell Death & Disease*. **2**. e235.

[64] Tong, H., Yin, H., Hossain, M.A., Wang, Y., Wu, F., Dong, X., et al. (2019) Starvation-induced autophagy promotes the invasion and migration of human bladder cancer cells via TGF-β1/Smad3-mediated epithelial-mesenchymal transition activation. *Journal of Cellular Biochemistry*. **120**. 5118–5127.

[65] Migeon, J.C., Thomas, S.L., and Nathanson, N.M. (1995) Differential coupling of m2 and m4 muscarinic receptors to inhibition of adenylyl cyclase by Gi alpha and G(o)alpha subunits. *The Journal of Biological Chemistry*. **270**. 16070–16074.

[66] Duttaroy, A., Zimliki, C.L., Gautam, D., Cui, Y., Mears, D., and Wess, J. (2004) Muscarinic stimulation of pancreatic insulin and glucagon release is abolished in m3 muscarinic acetylcholine receptor-deficient mice. *Diabetes*. **53**. 1714–1720.

[67] Gautam, D., Han, S.-J., Heard, T.S., Cui, Y., Miller, G., Bloodworth, L., et al. (2005) Cholinergic stimulation of amylase secretion from pancreatic acinar cells studied with muscarinic acetylcholine receptor mutant mice. *The Journal of Pharmacology and Experimental Therapeutics*. **313**. 995–1002.

[68] Ji, B., Bi, Y., Simeone, D., Mortensen, R.M., and Logsdon, C.D. (2002) Human pancreatic acinar cells do not respond to cholecystokinin. *Pharmacology & Toxicology*. **91**. 327–332.

[69] Shin, Y.-H., Jin, M., Hwang, S.-M., Choi, S.-K., Namkoong, E., Kim, M., et al. (2015) Epigenetic modulation of the muscarinic type 3 receptor in salivary epithelial cells. *Laboratory Investigation; a Journal of Technical Methods and Pathology*. **95**. 237–245.

[70] Zhao, Q., Yue, J., Zhang, C., Gu, X., Chen, H., and Xu, L. (2015) Inactivation of M2 AChR/NF-κB signaling axis reverses epithelial-mesenchymal transition (EMT) and suppresses migration and invasion in non-small cell lung cancer (NSCLC). *Oncotarget*. **6**. 29335–29346.

[71] Niebergall-Roth, E. and Singer, M. V. (2003) Control of pancreatic exocrine secretion via muscarinic receptors: Which subtype(s) are involved?: A review. *Pancreatology*. **3**. 284–292.

[72] Mesnier, D. and Banères, J.-L. (2004) Cooperative conformational changes in a G-protein-coupled receptor dimer, the leukotriene B(4) receptor BLT1. *The Journal of Biological Chemistry*. **279**. 49664–49670.

[73] Feng, Y., Hu, X., Liu, G., Lu, L., Zhao, W., Shen, F., et al. (2018) M3 muscarinic acetylcholine receptors regulate epithelial-mesenchymal transition, perineural invasion, and migration/metastasis in cholangiocarcinoma through the AKT pathway. *Cancer Cell International*. **18**. 173.

[74] Marinissen, M.J. and Gutkind, J.S. (2001) G-protein-coupled receptors and signaling networks: emerging paradigms. *Trends in Pharmacological Sciences*. **22**. 368–376.

[75] Quinn, S., Flakes, T., Holcomb, E., Chavez, L., and Sabbatini, M. (2015) The Lack of Adenylyl Cyclase 1 Impairs the Inhibitory Effects of cyclic AMP on Cell Migration and Proliferation in Pancreatic Cancer. *The FASEB Journal*. **29**. 856.2.

[76] Lorenz, R., Aleksic, T., Wagner, M., Adler, G., and Weber, C.K. (2008) The cAMP/Epac1/Rap1 pathway in pancreatic carcinoma. *Pancreas*. **37**. 102–103.

[77] Zimmerman, N.P., Roy, I., Hauser, A.D., Wilson, J.M., Williams, C.L., and Dwinell, M.B. (2015) Cyclic AMP regulates the migration and invasion potential of human pancreatic cancer cells. *Molecular Carcinogenesis*. **54**. 203–215.

[78] O'Hayre, M., Vázquez-Prado, J., Kufareva, I., Stawiski, E.W., Handel, T.M., Seshagiri, S., et al. (2013) The emerging mutational landscape of G proteins and G-protein-coupled receptors in cancer. *Nature Reviews. Cancer*. **13**. 412–424.

[79] Spalding, T.A., Burstein, E.S., Wells, J.W., and Brann, M.R. (1997) Constitutive activation of the m5 muscarinic receptor by a series of mutations at the extracellular end of transmembrane 6. *Biochemistry*. **36**. 10109–10116.

[80] Poulin, B., Butcher, A., McWilliams, P., Bourgognon, J.-M., Pawlak, R., Kong, K.C., et al. (2010) The M3-muscarinic receptor regulates learning and memory in a receptor phosphorylation/arrestin-dependent manner. *Proceedings of the National Academy of Sciences of the United States of America*. **107**. 9440–9445.

[81] Resende, R.R. and Adhikari, A. (2009) Cholinergic receptor pathways involved in apoptosis, cell proliferation and neuronal differentiation. *Cell Communication and Signaling : CCS*. **7**. 20.

[82] Yule, D.I., Essington, T.E., and Williams, J.A. (1993) Pilocarpine and carbachol exhibit markedly different patterns of Ca2+ signaling in rat pancreatic acinar cells. *American Journal of Physiology-Gastrointestinal and Liver Physiology*. **264**. G786–G791.

[83] Figueroa, K.W., Griffin, M.T., and Ehlert, F.J. (2009) Selectivity of agonists for the active state of M1 to M4 muscarinic receptor subtypes. *The Journal of Pharmacology and Experimental Therapeutics*. **328**. 331–342.

[84] Keely, S.J., Calandrella, S.O., and Barrett, K.E. (2000) Carbachol-stimulated transactivation of epidermal growth factor receptor and mitogen-activated protein kinase in T(84) cells is mediated by intracellular Ca2+, PYK-2, and p60(src). *The Journal of Biological Chemistry*. **275**. 12619–12625.

[85] Shafer, S.H. and Williams, C.L. (2004) Elevated Rac1 activity changes the M3 muscarinic acetylcholine receptor-mediated inhibition of proliferation to induction of cell death. *Molecular Pharmacology*. **65**. 1080–1091.

[86] Yan, Y., Hein, A.L., Etekpo, A., Burchett, K.M., Lin, C., Enke, C.A., et al. (2014) Inhibition of RAC1 GTPase sensitizes pancreatic cancer cells to γ-irradiation. *Oncotarget*. **5**. 10251–10270.

[87] You, Y., Kim, J., Cobb, M., and Avery, L. (2006) Starvation activates MAP kinase through the muscarinic acetylcholine pathway in Caenorhabditis elegans pharynx. *Cell Metabolism*. **3**. 237–245.

[88] Sugita, S., Uchimura, N., Jiang, Z.G., and North, R.A. (1991) Distinct muscarinic receptors inhibit release of gamma-aminobutyric acid and excitatory amino acids in mammalian brain. *Proceedings of the National Academy of Sciences of the United States of America*. **88**. 2608–2611.

[89] Onali, P., Dedoni, S., and Olianas, M.C. (2018) M3 Muscarinic Acetylcholine Receptors Inhibit Autophagy through Activation of mTORC1 in Human Neuroblastoma Cells. *The FASEB Journal*. **31**. lb569–lb569.

[90] Phillips, P.A., Yang, L., Shulkes, A., Vonlaufen, A., Poljak, A., Bustamante, S., et al. (2010) Pancreatic stellate cells produce acetylcholine and may play a role in pancreatic exocrine secretion. *Proceedings of the National Academy of Sciences of the United States of America*. **107**. 17397–17402.

[91] Razani-Boroujerdi, S., Behl, M., Hahn, F.F., Pena-Philippides, J.C., Hutt, J., and Sopori, M.L. (2008) Role of muscarinic receptors in the regulation of immune and inflammatory responses. *Journal of Neuroimmunology*. **194**. 83–88.

[92] Best, M.G., Sol, N., Kooi, I., Tannous, J., Westerman, B.A., Rustenburg, F., et al. (2015) RNA-Seq of Tumor-Educated Platelets Enables Blood-Based Pan-Cancer, Multiclass, and Molecular Pathway Cancer Diagnostics. *Cancer Cell*. **28**. 666–676.

Acknowledgements

I would like to thank…

Prof. Dr. med. Jens Werner for providing me the opportunity to go to Germany for doing research in such a lovely lab. The cordial interaction with you during the annual conference and the presentations meeting bring me the feeling of being included and accepted. This do helps to building up my self-confidence and the feeling of presence during the ups and downs in these years of research.

PD Dr. Bernhard Renz for the opportunity to work on this project and introducing me to such fantastic research about the relationship between cancer and the nerve system. Without a doubt, this is a wonderful enlightenment to the scientific research world. Thank you for giving me the freedom to think independently and critically although as a fresh researcher many of my conviction were naive. As a surgeon with heavy workloads, you always kept the spirit of scientific exploration and stayed active and rigorous with academics. This will always inspire me in my future professional career about not only being a doctor who can give treatment but also as a clinic scientist who makes his contributions to striving for better treatment options and clinic scientific progression. There are so many details, make it brief, thank you for all the kind support.

Prof. Dr. Alexandr Bazhin for all the kind support during my research in all these years. Thank you so much for giving me the room to think independently and to explore my interests. You are so considerate and liberal, this brings me the courage in so many difficult time points I was going through and bring me to this far. Your tolerance helped me to find the courage to persevere despite an existential crisis. This is not an exaggeration and I will always hold on to this gratitude. Thank you again from the bottom of my heart.

PD Dr. Barbara Mayer, thank you for all the optimistic atmosphere, this kills so many depressing and even lonely times for me. Maybe you're just used to working late, but I feel as if I'm being kept company, and that's a really good feeling.

All the kind members of the lab, especially Dr. Serene Lee, Sevdije Issar Amerchel, and Nicole Sylvia Strobl.

All the fellow students and former colleagues who bring kindly advise and support especially Dr. Sisi Lin, Dr. Zhiqiang Li, Dr.Chen Chen, Dr. Jing Wang. Dr. Hao Feng, Dr. Jingkun Zhao.

China Scholarship Council for honoring me with the scholarship.

My parents, for supporting me all the time, and the understanding and tolerance to me when I am straggling with my bad days. As the ‘’forever’’ kid in your heart, thank you for restraining your worries and still give me the freedom to make my own choice about my future, even this means separation and adventure. Please do not worry, distance does not diminish the love between us. I am a more sophisticated person now.

My dear Grandma Shuxian Lan for teaching me how to be tolerant, steadfast, and stay optimistic about the future even when life is hard. I would always be so proud to be a clinic doctor as you were. It’s a great regret and pity for me to miss the chance to say goodbye but I know in heaven you are amiably gazing and blessing me like always.

Myself, the brave small city girl who boarded the plane and say yes without any doubt not only to the over ten hours long trip but also to all the unpredictable in life.

Affidavit

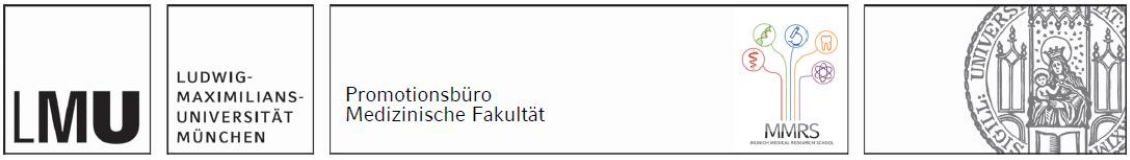

Affidavit

Qian, Li

Surname, first name

Street

Zip code, town, country

I hereby declare, that the submitted thesis entitled:

Role of Muscarinic Signalling in Pancreatic Cancer

is my own work. I have only used the sources indicated and have not made unauthorized use of services of a third party. Where the work of others has been quoted or reproduced, the source is always given.

I further declare that the submitted thesis or parts thereof have not been presented as part of an examination degree to any other university.

Nuremberg, 22.12.2022 — Qian Li

place, date — Signature doctoral candidate